Archimer
https://archimer.ifremer.fr

A threefold perspective on the role of a pockmark in benthic faunal communities and biodiversity patterns

Sánchez Nuria [1, *], Zeppilli Daniela [1], Baldrighi Elisa [1], Vanreusel Ann [2],
Gasimandova Lahitsiresy Max [1], Brandily Christophe [1], Pastor Lucie [1], Macheriotou Lara [2],
García-Gómez Guillermo [3], Dupré Stephanie [4], Olu Karine [1]

[1] Institut Français de Recherche pour l'Exploitation de la MER (IFREMER), Laboratoire Environnement Profond, France
[2] Marine Biology, Ghent University, Belgium
[3] School of Environment Sciences Earth, Ocean & Ecology Sciences Department, University of Liverpool, UK
[4] Institut Français de Recherche pour l'Exploitation de la MER (IFREMER), Unité Géosciences Marines, France

* Corresponding author : Nuria Sanchez, email address : Nuria.Sanchez.Santos@ifremer.fr

---

Abstract :

Pockmarks are circular-shaped depressions that increase seabed heterogeneity and are characterized by discontinuous fluid emissions. To understand how environmental conditions of pockmarks affect the structure of macro- and meiofauna, we investigated two sites in a pockmark field in the northwestern Madagascar margin. In a comparative approach, we explored the community structure of the dominant taxa (Polychaeta, Nematoda and hyaline foraminifera) in each component (macro-, metazoan meiofauna and foraminifera, respectively). The investigated active pockmark showed approximately two times higher meiofauna abundance compared to in a site away from another pockmark field, but macrofauna showed the opposite trend, with almost half density at the pockmark site. However, at both sites, macro- and meiofauna showed higher richness and abundance values in the top well-oxygenated layers of the sediment than in the underlaying ones. Polychaeta and Nematoda showed lower richness in the pockmark, opposed to hyaline foraminiferans, but lower evenness in the pockmark was found for the three groups. The detection of gas flares in the water column attests of the recent activity within the pockmark. High amount of sulfur-bearing minerals (mainly pyrite) evidences a production of dissolved free sulfides (not detected at the time of sampling) by sulfate reduction process driven by organic matter degradation and anaerobic oxidation of methane. Furthermore, recent increase in sedimentation rates in the past 70 years and organic matter inputs could have led to higher organic matter degradation rates resulting in reduced conditions and a high oxygen consumption. All this together seem to act as key factors in the determination of variation in richness, abundance and community composition of macrofauna and meiofauna. Additionally, some taxa seem to be more tolerant to these extreme conditions, such as species belonging to the Nematoda genus Desmodora and the phylum Kinorhyncha, which are highly abundant in the pockmark, and hence, may be considered as potential bioindicators of pockmark activity in this area. Further studies are required for a better assessment.

Highlights

► Environmental conditions of pockmarks affect benthic community composition. ► Meiofaunal taxa are able to take advantage of pockmark activity, i.g *Desmodora*. ► *Desmodora* nematode could be a benthic indicator of fluid emission. ► Benthic community compositions are largely dissimilar between the two sites.

1. Introduction

Deep-sea floor exploration has revealed vast geological, chemical, and biological heterogeneity on continental margin ecosystems (Levin and Sibuet, 2012; Menot et al., 2010). Among them, pockmarks specifically refer to circular/ellipsoid depressions in the seabed which increase seafloor heterogeneity as they represent habitats with high structural complexity where fluid emission can vary in space and time (Dando et al., 1991; Hovland and Judd 1988). Organisms inhabiting in active pockmarks are able to cope with the conditions that can characterize this kind of environments, such as high concentrations of reduced chemical compounds, low oxygen levels, and high primary production based on chemoautotrophic bacteria (Levin, 2005; Sibuet and Olu, 1998; Zeppilli et al., 2018).

The presence of specific macrofaunal communities (organisms > 1 mm length) can serve as a valuable tool for identifying the various habitats created by gas emissions. In particular, some Polychaeta families, such as Ampharetidae, Hesionidae, Capitellidae or Dorvilleidae, are adapted to sulphide-rich and hypoxic sediments and therefore dominate such environments (Decker et al., 2012; Donnarumma et al., 2019; Guillon et al., 2017; Levin, 2005; Menot et al., 2010; Portail et al., 2015; Rouse and Fauchald, 1997; Rouse and Pleijel, 2001). In contrast, deep-sea meiofaunal communities, both metazoan and foraminifera (pluricellular and unicellular organisms < 1 mm length, respectively), have been historically less investigated in these habitats, although they can also be used as benthic indicators of changes in environmental conditions (Table 1 in Zeppilli et al., 2015) due to their rapid generation time and the lack of larval dispersion in the dominant groups (Giere, 2009). Moreover, several studies have shown that specific taxa, such as Draconematidae and Monhysteridae nematodes, Darcythompsoniidae and Dirivultidae copepods (Table 1 in Zeppilli et al., 2018 for detailed information), can tolerate or even thrive in extreme environmental conditions, such as high levels of hydrogen sulfide or hypoxia, where most species cannot survive (Baldrighi et al., 2020a; Gooday et al., 2009; Levin, 2003; Van Gaever et al., 2006).

3

75   To date, few studies assessed the response of both deep-sea macrofauna and metazoan

76   meiofauna to cold fluid emission simultaneously, showing similar patterns for diversity in both

77   communities, but opposite trends or little differences compared to background sediments for

78   density (Ritt et al., 2010; Van Gaever et al., 2009a and references therein), and no

79   comparative study includes foraminiferal fauna. In the present study, we investigated the

80   distribution and diversity patterns of benthic fauna using an integrative ecological approach

81   including macrofauna and meiofauna from the Majunga Basin in the northwestern

82   Madagascar margin (Mozambique Channel) (Fig. 1a). In this area, pockmark clusters were

83   recently discovered along the slope, front of two main Mahavavy Sud and Betsiboka rivers,

84   given rise to a serial of multidisciplinary sampling campaigns in the framework of PAMELA

85   project (Dupré et al., 2019; Jorry, 2014; Olu, 2014). Foraminifera community structure and

86   their paleoenvironmental application were previously investigated in the referred area

87   (Fontanier et al., 2016; 2018), showing extremely elevated diversity in areas characterized by

88   high concentrations of degraded organic matter and moderate oxygen penetration in the

89   seafloor (15 and 30 mm), while areas of reduced oxygen penetration showed lower diversity

90   (Fontanier et al., 2016). The foraminifera dataset of this paper will be used for the

91   comparison between sites and with the other benthic components. Since our study is part of

92   a large multidisciplinary project, more stations and samples were investigated for other

93   purposes, but samples of the three benthic components were only collected at two sites.

94   Therefore, a complete data set that allow the comparison among the three faunal

95   components is only available from these two sites: one within an active pockmark and

96   another one located away from pockmarks. The main goals of our study were to: 1)

97   characterize and compare macrofauna, metazoan meiofauna and foraminifera benthic

98   communities in the referred two sites; 2) discuss the effect of environmental constraints on

99   the distribution and diversity of the three aforementioned benthic components; and 3)

100   evaluate the reliability of key most dominant taxa (i.e. Polychaeta, Nematoda and Hyaline) at

101   the upper most sediment layer (0-1 cm, which usually host vast majority of benthic

102   organisms) as potential indicators of pockmark activity.

103

2. Materials and methods

2.1. Seepage exploration and study sites

The study area was selected based on previous samples of bivalves usually associated with cold seeps (Bathymodiolinae shells and living Vesicomyidae) and collected during the MIRIKI cruise (2009) (P. Bouchet, pers. comm.). Our sampling sites (Fig. 1b) were chosen based on geophysical data (seismics, bathymetry and seafloor backscatter data and acoustic imagery of the water column) of the Ptolemée and Pamela-Moz01 cruises (Jorry, 2014; Olu, 2014) and seabed inspection with the deep-towed camera Scampi to locate cold seeps (e.g. reduced sediment, bivalves, microbial mats) (Olu, 2014; Dupré et al., 2019). Multibeam echosounder surveys were conducted during these marine expeditions with the use of a EM122 ship-borne multibeam echosounder operated at 12 kHz. Seafloor bathymetry (Figs. 1b and 1c) and acoustic imagery of the water column (Fig. 1c) were acquired offshore northwestern Madagascar in the Majunga Basin. Given the impedance contrast between the ambient seawater and gas bubbles, water column echosounder data record acoustic anomalies caused by the presence of gas bubbles, providing thus crucial information on potential active seeping sites (Dupré et al. 2015). Two sites located on Betsiboka and Mahahavy Sud slopes (ca. 30 km apart) were chosen for faunal sampling with samples collected inside an active pockmark and away from another pockmark field. Nevertheless, all three faunal components were only analyzed at two sampling points (Table 1; Fig. 1). At Site 1 on the Mahavavy Sud slope, samples were specifically collected within an active pockmark (600 m of diameter), at c.a. 780 m water depth. At Site 2 on the Betsiboka slope, samples were taken outside another pockmark field, at c.a. 529 m water depth.

2.2. Regional settings

The large pockmark sampled at Site 1 (600 m diameter) presented a marked shift in sediment accumulation rates around the 1950s (Fontanier et al., 2018), with values similar to

129   the rest of the continental slope before that (around 0.04-0.06 cm yr-1 - Pastor et al., 2020),

130   and much higher values during the last 70 years (0.25 cm yr-1 - Fontanier et al., 2018)

131   representing the 0-16 cm layer. This pulsed sedimentation was interpreted as two or three

132   main input events over the last 70 years (Fontanier et al., 2018), favored by episodic

133   reconnection of the Mahavavy Sud River with the canyon head during extreme climatic

134   events (Pastor et al., 2020). These events brought high loads of relatively degraded organic

135   matter as shown by low enzymatically to total hydrolysable amino acid ratios (EHAA/THAA

136   ratio; Fontanier et al., 2018). This surficial layer is also characterized by a very high

137   accumulation of total sulfur, most certainly *in situ* formed pyrite due to the pulsed high loads

138   of organic matter, its degradation by sulfate reducers, and concomitant high concentration of

139   iron oxides (Pastor et al, 2020). These pulsed episodes seemed to be also responsible for a

140   shift in foraminifera communities (Fontanier et al., 2018).

141   Sampling in Site 2 occurred about 3.5 km away from the closest active pockmark field, at

142   slightly shallower water depths. In this area, sediment accumulation rates reflected a very

143   low input of particulate matter from the Betsiboka River (Pastor et al., 2020).

144   *2.3. Sediment sampling and processing*

145   Following the recommendations of Montagna et al. (2017), only one replicate sample per

146   station with pseudoreplicated cores were collected. Macrofauna was sampled using USNEL

147   box corers (KGS), subsampled three times with blade corers (surface= 0.018 m²).

148   MOZ01KGS03 was collected on the Mahavavy Sud slope (Site 1); and MOZ01KGS01 on the

149   Betsiboka slope (Site 2). USNEL blade cores for macrofauna were sliced horizontally in five

150   layers to 15 cm depth (0-1, 1-3, 3-5, 5-10, 10-15 cm). Each layer was sieved through 1 mm,

151   500 µm and 300 µm mesh size sieves. Samples for morphological studies were fixed

152   onboard in 4% formalin for 24 h and then transferred to 90% ethanol. Macrofaunal animals

153   were sorted and identified to major taxonomic levels (phylum/class/subclass/order/family)

154   using a binocular stereomicroscope Leica M125. Only macrofauna *sensu stricto* (Hessler and

Jumars, 1974) were included, and typical meiofaunal taxa such as Nematoda and Copepoda were excluded from these samples. Macrofaunal Polychaeta in the first sediment layer (0-1 cm) were identified to the family level using a binocular stereomicroscope Leica M125.

Metazoan meiofauna were sampled using a multi-corer (Barnett-type, MTB), with a total of three cores from the same deployment (62 mm of internal diameter) at each site. MOZ01MTB06 samples were collected at Site 1 near the center of the pockmark; and MOZ01MTB01 was collected at Site 2 (both deployments suffered of common minor variations from the GPS points of the macrofauna sampling due to sampling environmental conditions; see Table 1). Cores for metazoan meiofaunal studies were sliced on board horizontally in 5 layers (0-1, 1-2, 2-3, 3-4, 4-5 cm), and subsequently fixed in 4% formalin. The sediment of each slice was sieved on 1 mm and 32 µm mesh size sieve; animals were extracted from the sediment using Ludox centrifugation (Heip et al., 1985) and then sorted and identified using a binocular microscope Leica MZ 8 to the higher taxonomic levels typically used for meiofaunal studies (phylum/class/subclass/order/family) (Danovaro, 2010). Additionally, approximately 100 nematodes from the first sediment layer (0-1 cm) of each core were mounted on slides and identified to genus level using a microscope Leica DM2500 LED. The foraminifera community was sampled from two cores (62 mm of internal diameter) at each site, MOZ01MTB07 at Site 1 and MOZ01MTB01 at Site 2 (deployments were displaced a few meters away of the GPS points of the macrofaunal sampling, as already referred for the metazoan meiofauna samplings; see Table 1). In the present study, we used the identification dataset to species level generated by Fontanier et al. (2016) to cluster the specimens in the main foraminifera groups: hyaline, agglutinated, porcelaneous and soft-shell foraminifera (see the referred publication for detailed information on sampling procedure and identification of alive specimens).

Oxygen profiles were measured *ex situ* using Clark-type electrodes as described in Pastor et al. (2011). Organic Carbon (OC) was measured on freeze-dried and crushed sediment after removal of carbonates with 2 M HCl using an automatic ThermoFinnigan EA1112 Series

182   Flash elemental analyzer. Total sulfur was measured on the same powdered samples using

183   a LECO CNS-2000 auto-analyzer. On-board measurements of H_2S were based off the Cline

184   method (Cline 1969; Grasshoff et al., 1999) and the absorbance was read at 670 nm (Pastor

185   et al., 2020).

186   *2.4. Faunal data and statistical analysis*

187   Macrofauna, metazoan meiofauna and foraminifera community descriptors were: (1)

188   richness, (2) abundance and (3) taxonomic composition. We used the same community

189   descriptors for Polychaeta, Nematoda and hyaline foraminifera, considering only the

190   uppermost 0-1 cm of the vertical profile because it is the single layer for which we obtained a

191   complete dataset and which allows a comparable study among the three groups (cores for

192   macrofauna were sliced at different depths than those for meiofauna). Richness was

193   measured as the number of high-taxonomic-level taxa of the macrofaunal, metazoan

194   meiofaunal and foraminifera communities. In addition, we used the number of families for

195   Polychaeta, the number of genera for Nematoda, and the number of species for hyaline

196   foraminifera. Abundance was measured as the number of individuals in a core sample and

197   densities were calculated as the number of individuals per surface area (1 m^2 for macrofauna

198   and Polychaeta, 10 cm^2 for metazoan meiofauna, foraminifera, Nematoda and hyaline

199   foraminifera). Statistics were based on pseudoreplicates, which explain larger spatial

200   variance of richness and abundance than true replicates do according to Montagna et al.

201   (2017). Hence, analyses of each benthic component were performed using the faunistic data

202   from all cores collected at each site, considering them as independent units.

203   Differences in taxa richness and abundance were described along the vertical profile within

204   each site (intra-site study) for macrofauna (0-1, 1-3, 3-5, 5-10, 10-15 cm), metazoan

205   meiofauna (0-1, 1-2, 2-3, 3-4, 4-5 cm) and foraminifera (0-1, 1-2, 2-3, 3-4, 4-5, 5-6, 6-7, 7-8,

206   8-9, 9-10 cm). Layer 0-1 of core MOZ01MTB6-A used for metazoan meiofauna studies was

207   excluded due to processing problems that resulted in the loss of most animals. Then, we

208 tested for the effect of the pockmark occurrence on the fauna (inter-site study). Generalized

209 Linear Models (GLMs) and Generalized Linear Mixed-effect Models (GLMMs) were chosen

210 to assess for faunal differences between the sites, instead of non-parametric analysis,

211 because they allow to make assumptions about the distribution of our data. Therefore, after

212 verifying data distribution of richness and abundance, models were implemented following

213 Poisson and Gaussian (after logarithmic transformation of the abundance data) distributions,

214 respectively (Crawley, 2012). GLMMs were conducted to test for differences in richness and

215 abundance of macrofauna, metazoan meiofauna, and foraminifera between the two sites (1

216 and 2, Fig. 1b), using the site as a discrete explanatory variable (i.e. inter-site study),

217 including the variables of "sediment depth" and "core" as random factors. Similarly, GLMs

218 were performed considering only the 0-1 cm layer for the following taxa: family for

219 Polychaeta, genera for Nematoda and species for hyaline foraminifera. GLMs and GLMMs

220 were conducted using the 'glm', 'lmer' and 'glmer' functions implemented in R (Zuur et al.,

221 2007). Polychaeta, Nematoda, and hyaline foraminifera diversities were measured using the

222 Shannon–Wiener diversity index (H', log-base e) with the Pielou index (J) for evenness,

223 using the 'diversity' function included in the R package vegan v. 2.2-1 (Oksanen et al., 2015).

224 Differences in community composition were tested using Ružička matrix with a permutational

225 analysis of variance models (PERMANOVA). Ružička index were calculated using the 'beta'

226 function of the R package vegan v. 2.2-1 (Oksanen et al., 2015), and PERMANOVA was

227 performed using the 'adonis' function included in the R package vegan v. 2.2-1 (Oksanen et

228 al., 2015).

229 To visualize community structure variations between sites in macrofauna, metazoan

230 meiofauna, and foraminifera as well as in Polychaeta, Nematoda, and hyaline foraminifera,

231 we conducted a Principal Component Analysis (PCA) on abundance using the 'rda' function

232 of the R package vegan v. 2.2-1 (Oksanen et al., 2015). Abundance data were transformed

233 (Hellinger distance) using the 'decostand' function of vegan 2.5-5 package (Oksanen et al.,

234 2018), because this distance gives a lower weight to dominant taxa and does not consider

235 double absence as an indicator of similarity between samples (Legendre and Gallagher,

236 2001). A post hoc test of the PCA axes was performed by the function 'envfit' of the R

237 package vegan 2.4-4 (Oksanen et al., 2018).

238

239 **3. Results**

240 *3.1 Water column acoustic data*

241 At the pockmark of Site 1, seepage activity, although of relatively low intensity, was

242 evidenced based on acoustic water column data (Fig. 1c). At this area, some of the water

243 column echoes identified in 2D polar echograms were rooted in the seabed and interpreted

244 as escaping gas bubbles, most likely composed of methane. In contrast, Site 2 located away

245 from another pockmark field was not characterized by methane seepage, at least at the time

246 of the survey. No active pockmarks have been reported in the close vicinity of Site 2, the

247 closest inactive pockmark being distant from more than 600 m.

248 *3.2 Geochemical settings*

249 In the recovered sediment at Site 1, dissolved oxygen was consumed within 17.5 mm, no

250 dissolved free sulfide ($\sum H2S = S2- + HS- + H2S$) was detected and methane ($CH4$) was < 1

251 µM, organic carbon concentrations were around 2.0% (Pastor et al., 2020; this study) (Annex

252 I).

253 At Site 2, OC contents were lower than in Site 1 reaching 1.1 %, and even more degraded

254 with EHAA/THAA lower than 10% (Fontanier et al., 2016). O_2 penetration depth was around

255 30 mm. No CH_4 was detected and a peak of $\sum H_2S$ of 34 µM at 11 cm depth was measured

256 (Pastor et al., 2020; this study) (Annex I).

257

258 *3.3. Macrofaunal community*

3.3.1. Intra-site

Abundances at Site 2 (away from the pockmark field) showed similar high values at the two uppermost sediment layers but decreasing gradually with sediment depth (ca. 30% of the fauna in 0-1 cm; ca. 32% in 1-3 cm) (Table 2; Annex II). Most taxa showed a similar trend, except Polychaeta, whose abundance at Site 2 reached a peak at layers 1-3 and 5-10 cm (Fig. 2). At Site 1 (inside the active pockmark), total macrofaunal abundance was high in the first centimeter, with ca. 75% of the total abundance, and much lower in the deeper layers (Table 2; Fig. 2; Annex II); taxa abundance showed a similar pattern. At Site 2, richness was the highest in the surface layers down to 3 cm depth, decreasing only in the layers below 3 cm (from 6.0 ± 1.0 and 5.5 ± 1.2 in layers 0-1 and 1-3 cm, respectively, to 2 ± 0 at 10-15 cm) (see Table 2; Annex II). At Site 1, most of the richness was present in the uppermost sediment layer (0-1 cm, 5.3 ± 0.6), with a maximum of two taxonomic groups per layer below the surface (Table 2; Annex II). The community along the vertical profile at the two study sites was dominated by Polychaeta from the upper to the lower layers (Fig. 2), with one single exception: Nemertea was the dominant taxon in layer 5-10 cm at Site 1 (ca. 74% of the macrofauna community in this layer). Peracarid crustaceans (Isopoda, Tanaidacea, Cumacea, and Amphipoda) were relatively abundant (ca. 52%) in layer 0-1 cm at Site 2.

3.3.2. Inter-site

Overall macrofauna abundance was higher at Site 2, with 99 ± 7 specimens per core at Site 2 and 60 ± 35 at Site 1 (GLM, $P< 0.05$; Annex III) (Table 3). Polychaeta dominated both sites, accounting for ca. 61% and ca. 49% of the overall abundance at Sites 2 and 1, respectively. Aplacophora, Nemertea, and Bivalvia abundances reached higher values at Site 1 than at Site 2 (ca. 17% at Site 1 vs. 1.7% at Site 2; 10% at Site 1 vs. 1.3% at Site 2; 8% at Site 1 vs. 2.7% at Site 2, respectively), and Cumacea was only found at Site 2 (Table 3; Fig. 2). For the most abundant taxonomic groups (greater than 5% of the total community at one site), the analysis confirmed variation between sites in Polychaeta, Cumacea, Tanaidacea, and Amphipoda (see Annex III). Significant differences in richness between the

286   two study sites were found as well, with 8.7 ± 1.5 taxa at Site 2 and 7.0 ± 1.0 at Site 1 (GLM,

287   $P < 0.01$; Annex III) (Table 3; Fig. 3; Annex II).

288   According to the PERMANOVA analysis, the "site" factor significantly affected the shifts

289   between the two study sites ($P = 0.005$; Annex III). PCA conducted on abundances

290   discriminated faunal composition between the two sites. PC1 explained 54.7% of the

291   variance and was mainly affected by the high abundance of Cumacea at Site 2, and those of

292   Aplacophora and Nemertea affected Site 1 (Fig. 4).

3.3.3. Polychaeta community

294   In the first sediment layer, differences in abundance between the two sites were not

295   statistically significant, with 12 ± 10 specimens per core at Site 2 and 23 ± 12 at Site 1 (GLM,

296   $P > 0.05$; Annex III; Table 4; Fig. 6). The dominant family at both sites was Spionidae

297   representing ca. 39% and 35% of the community at Sites 1 and 2, respectively (Table 4; Fig.

298   5). At Site 1, inside the active pockmark, Hesionidae and Cossuridae were also abundant

299   (ca. 25% and 18% of the Polychaeta fauna, respectively), followed by Polynoidae and

300   Capitellidae (ca. 12% and 7%). At Site 2, away from the pockmark field, Syllidae was the

301   second most dominant family after Spionidae (ca. 19%) and its presence in Site 1 was

302   restricted to a singleton (Table 4; Fig. 5). Abundance of the remaining families was extremely

303   low (Fig. 5). Opheliidae were only present at Site 2 (ca. 14%) (Table 4; Fig. 5). Hesionidae,

304   Cossuridae, Polynoidae, and Capitellidae were only found at Site 1. Analyses performed for

305   each family only found statistically significant changes for the Hesionidae (GLM, $P < 0.001$;

306   Annex III). Richness and diversity also had similar values at both sites (5.3 ± 2.5 families at

307   Site 2 and 4.3 ± 0.6 families at Site 1, GLM, $P > 0.05$; Annex III; H' 1.8 and 1.6; J' 0.8 and 0.8,

308   respectively) (Table 4; Fig. 6). PCA conducted on abundance revealed a strong

309   discrimination in family composition between sites. PC1 explained 47.5% of the variance and

310   was mostly affected by the high densities at Site 1 of Cossuridae, Hesionidae, Polynoidae;

311   whereas the high abundance of Opheliidae characterized Site 2 (Fig. 4).

312

3.4. Metazoan meiofauna community

3.4.1. Intra-site

Total abundance along the vertical profile was higher at the second layer of the sediment (ca. 47% at both sites) (Table 2; Annex II). Nematoda were the dominant taxa in each layer (> 78% of the community in all layers at Site 2, and > 82% in all layers at Site 1), followed by Copepoda (Fig. 2). At Site 2, abundances strongly decreased from the third layer, comprising ca. 30% of the community, about three times higher than in the uppermost centimeter (Table 2, Annex II). All taxa abundances followed this pattern except for Polychaeta, which showed similar abundances down to the fourth layer (Fig. 2). Similar patterns were observed at Site 1, inside the active pockmark, although the decrease in abundance in the third sediment layer (2-3 cm) was even more drastic, from ca. 47% down to 16% (Table 2, Annex II). Kinorhyncha increased in the second layer at Site 1, from 1.3% to 3.6% at 1-2 cm depth (Fig. 2). Gradual changes in richness along the vertical profile were observed at Site 2, with the highest values in the upper layers (8 ± 3 and 8 ± 1 taxa, respectively), and the lowest values in the bottom layers (5.3 ± 1.2 and 1 ± 1 taxa, respectively). At Site 1, most of the richness was in the uppermost sediment layers (10 ± 4 and 8 ± 2), decreasing down to 3-4 cm depth (Table 2, Annex II).

3.4.2. Inter-sites

Meiofauna were more abundant at Site 1, with 6041 ± 3337 versus 2643 ± 381 specimens per core at Site 2 (GLM, $P < 0.01$; Annex III), whereas both sites were similar in terms of richness, with 12.0 ± 2.7 taxa at Site 1 and 9.7 ± 1.2 at Site 2 (GLM, $P < 0.05$; Annex III; Table 5, Annex II). This pattern of general meiofaunal abundance was observed for most of the studied taxonomic groups, except for Polychaeta, Tantulocarida, Tardigrada, Platyhelminthes, and Isopoda. The main dominant taxa in each site was Nematoda (ca. 87% at Site 1, 92% at Site 2), followed by Copepoda (ca. 6% and 5%). Kinorhyncha, which were

338 almost absent at Site 2, ranked third in abundance at Site 1, representing up to 2.7% of the

339 meiofauna (Table 5; Fig. 2). Other taxa were recovered in one or the other site in low

340 numbers: Tantulocarida, Platyhelminthes, and Isopoda at Site 2; Amphipoda, Aplacophora,

341 Cnidaria, Gastropoda, and Halacarida at Site 1 (Table 5; Fig. 2). Analyses of the three most

342 abundant groups (greater than 5% of the total community at any one site), revealed statistical

343 differences between the two sites for Nematoda and Kinorhyncha (GLM, $P< 0.01$ and $P<$

344 0.01 respectively; Annex III).

345 According to the PERMANOVA results, the "site" parameter had a significant effect ($P< 0.05$;

346 Annex III). PCA visualizing the trends of the meiofauna community composition in terms of

347 abundance discriminated between the two study sites due to PC1, which explained 57.4% of

348 the variance and was mainly affected by the high densities of Kinorhyncha, followed by

349 Nauplii at Site 1. PC2 explained 31% of the variance and was mostly affected by Copepoda

350 and Kinorhyncha (Fig. 4).

351 **3.4.3. Nematoda community**

352 The abundance in the 0-1 cm layer was higher at Site 1 than at Site 2, with 1888 ± 1806

353 specimens per core and 236 ± 88 specimens per core, respectively, but the differences were

354 only marginally significant (Table 6; Fig. 6). The most dominant taxa at Site 2 were *Tricoma*

355 (ca. 14%), *Desmoscolex* (ca. 9%), *Halalaimus* (ca. 7%), and *Pselionema* (ca. 6%), whereas

356 a single genus was dominant at Site 1, *Desmodora* (ca. 51% of the Nematoda community),

357 followed by *Halalaimus* (ca. 8%) (Table 6; Fig. 5). The genera *Pselionema* and *Desmodora*

358 were restricted to just one site, away from a pockmark field and inside an active pockmark,

359 respectively. The remaining genera represented together ca. 74% and 41% of the Nematoda

360 community at Site 2 and Site 1, respectively, but the contribution of each genus to total

361 abundance was always less than 5%. Analysis on the most abundant genera (above 5% of

362 the total community at any one site), only found statistically significant changes between the

363 two sites for *Desmodora* and *Pselionema* (GLM, $P< 0.001$ and $P< 0.01$ respectively; Annex

364 III). Moreover, Site 2 showed significantly higher genus richness and higher diversity than

365   Site 1, with 40 ± 11 and 19 ± 17 genera, respectively (GLM, *P*< 0.001; Annex III; H' 3.6 and

366   1.7; J' 0.8 and 0.5, respectively) (Fig. 6; Table 6).

367   PCA conducted on abundance revealed a strong difference in Nematoda composition

368   between the sites due to the abundance of *Tricoma* and *Pselionema* at Site 2 and the

369   exclusive presence and high abundance of *Desmodora* at Site 1. *Desmodora* abundance

370   strongly affected PC1, which explained 60.9% of the variance (Fig. 4).

371

372   *3.5. Foraminifera community*

373   **3.5.1. Intra-sites**

374   At both sites, the highest abundance along the vertical profile was found at the uppermost

375   sediment layer, with 609 ± 9 specimens per core at Site 2, and 1325 ± 989 specimens at Site

376   1 (Table 2; Annex II, Fig. 2). At Site 2, the decrease in abundance from the surface to the

377   deeper layers was steeper than at Site 1 (Table 2, Annex II). Similar patterns were observed

378   for main foraminifera groups and hyaline and agglutinated foraminifera dominated in each

379   layer regardless of site (Table 7).

380   **3.5.2. Inter-sites**

381   Changes in foraminifera abundance between sites were not significant, with means of 1956 ±

382   1059 and 839 ± 37 specimens per core at Site 1 and Site 2, respectively (Table 7; Annex II

383   and III). Hyaline foraminifera were dominant at both sites, followed by agglutinated,

384   porcelaneous and soft-shell foraminifera (Table 7, Fig. 2). The four main foraminifera groups

385   were present at both sites and no significant changes were detected. Considering each

386   group, richness was mostly due to the presence of hyaline foraminifera (42 ± 2.8 species at

387   Site 2 vs. 50 ± 14.8 at Site 1) and agglutinated foraminifera (50.5 ± 4.9 vs. 37 ± 12.7), and

388   the contributions were marginal for porcelaneous (ca. 13 ± 0.0 vs. 5.5 ± 2.1) and soft-shell

389   taxa (ca. 3.0 ± 1.4 vs. 1.0 ± 0.0). At Site 1, the hyaline foraminifera dominated along with

390 agglutinated foraminifera. Analysis performed on groups showed significant changes only in

391 soft-shell foraminifera abundance between sites (Annex III).

392 PERMANOVA performed on the four foraminifera groups did not reveal any significant

393 differences in the community structure of the two sites (Annex III). PCA did neither

394 discriminate between the two sites (Fig. 4).

3.5.3. Hyaline community

396 Variations in abundance and richness in layer 0-1 cm were not significant between sites, with

397 means of 736 ± 429 vs. 379 ± 44.5 specimens per core, and 49.5 ± 14.8 vs. 42 ± 2.8 species

398 at Site 1 and Site 2 respectively (see Annex III; Fig. 6 and Table 8 for details). Site 1 showed

399 slightly lower diversity than Site 2 (H' 2.6 and 2.9; J' 0.6 and 0.7, respectively). The species

400 *Bulimina marginata* and *Uvigerina hispida* were abundant at both sites, but the dominance of

401 *B. marginata* at Site 1 was not comparable to that of *U. hispida*: *B. marginata* ca. 28% of the

402 community followed by *Bolivina alata* ca. 24%, *Bulimina inflata* ca. 9%, and *U. hispida* ca. 5%

403 (208 ± 144, 173 ± 165, 63.5 ± 37.5, 37.5 ± 39, respectively) (see Table 8 and Fig. 5). Some

404 species were relatively abundant at Site 1, but absent at Site 2, such as *B. alata* (ca. 24%),

405 *Bolivina spathulata* (type 2) (ca. 6%) (173 ± 165 and 45.5 ± 19.1, respectively), and *B. inflata*

406 ranking third in abundance at Site 1 (ca. 9%, 63.5 ± 37.5) and mostly absent at Site 2;

407 *Uvigerina semiornata* was present as a singleton at Site 1 and in relatively high abundance

408 at Site 2 (ca. 11%, 43.5 ± 0.7) (see Table 8 and Fig. 5). At the species level (above 5% of the

409 total community at any one site), only changes in *U. semiornata*, *B. alata*, *B. spathulata* (type

410 2), and *B. inflata* were significant (see Annex III).

411 PCA conducted on abundances discriminated between the species composition of both sites

412 due to PC1 (73.4% of the variance), which was strongly affected by the high abundances of

413 *B. alata*, *B. spathulata* (type 2) and *B. inflata*, characterizing Site 1; *U. semiornata* and *U.*

414 *hispida* characterized Site 2 (Fig. 4).

415

4. Discussion

4.1. Are macrofaunal, metazoan meiofaunal and foraminifera communities similarly affected by pockmark occurrence?

Our results pointed that the three benthic communities were influenced by the environmental conditions, namely low oxygen availability and reduced conditions mainly due to high organic matter contents. Derived biological and geochemical processes linked to the presence of methane in the subseafloor as inferred from gas escapes within the pockmark (visible in acoustic water column data) could also influence the repartition of communities. Nevertheless, macro- and meiofauna were affected in different ways.

In our study, macrofauna abundance was significantly lower at the active pockmark (Site 1) compared to the site out of seep influence, in contrast to the meiofauna and foraminifera. Although high macrofaunal densities have been reported in some pockmarks (Decker et al., 2012; Guillon et al., 2017; Levin et al., 1991, 2003, 2010; Menot et al., 2010; Ritt et al., 2010; Sahling et al., 2002), opposite density patterns between meiofauna and macrofauna have been already observed in cold-seep environments, attributed to the sulfide gradient and biotic interactions between these two faunal compartments (see section 4.3) (Van Gaever et al., 2009a). The low macrofauna abundances can be explained by the reduced oxygen availability, usually concomitant to high H_2S levels (Decker et al., 2012; Guillon et al., 2017; Levin et al., 1991, 2003, 2010; Menot et al., 2010; Ritt et al., 2010; Sahling et al., 2002). Also, the vertical profile of fauna abundance was affected by the low oxygen penetration, following general fauna distribution patterns also shown in other pockmarks(Jensen, 1986; Montagna et al., 1989; Powell et al., 1983; Ritt et al. 2011), where organisms were concentrated in the upper centimeters within the pockmark but were more equally distributed along the vertical profile at site out of seep influence. According to Pastor et al. (2020), Site 2 was never impacted by any methane outflow, while sediment at Site 1 present clear geochemical imprints of methane circulation. The meter-scale spatial heterogeneity of these particular

442   areas, also evidenced by the Scampi video near-bottom surveys, most likely explain the very

443   low CH_4 and the absence of H_2S in our samples within the pockmark. It is worth noting that

444   the sampling, although in the close vicinity of gas emissions, are distant from them (i.e. c.a.

445   10 m for MOZ01MTB07, 30 m for MOZ01KGS03 and 50 m for MOZ01MTB06). The oxidation

446   of methane through migration towards surficial sediment layers, eventually forms sulfur-

447   bearing minerals such as pyrite (large amount of this sulfur-bearing minerals were detected

448   at Site 1 according to Pastor et al., 2020) and the process is partially or totally mediated by

449   anaerobic methanotrophic and sulfate-reducing bacteria (Boetius et al., 2000; Orphan et al.,

450   2001). Bacterial communities form a major food source for meiofauna which in turn could

451   explain their sizable densities in subsurface layers (Van Gaever et al., 2009a). On the other

452   hand, the high input in labile organic matter in the uppermost sediment layer (Fontanier et al.,

453   2016) could induce higher bacterial densities as well, which may explain the enhancement of

454   meiofauna population at the surface layer. Moreover, the significant higher abundances of

455   metazoan meiofauna in the pockmark indicated that at some sites, this benthic component

456   could better cope with more extreme conditions (Ritt et al., 2010), likely through replacement

457   with opportunistic specialized taxa that flourish in these environments (Vanreusel et al.,

458   2010). The relatively high heterogeneity found in meiofauna abundance among cores at Site

459   1 can be a result of diffusive methane taking multiple exit pathways through the pockmark

460   sediment even at the meter- scale corresponding to the area sampled by the multi-corer.

461   Richness of the three benthic components followed different patterns, and only macrofauna

462   showed lower richness in the active pockmark, as usually reported for seep communities

463   (Levin, 2005). Along the vertical profile, richness of the three components decreased more

464   gradually away from the pockmark due to greater dissolved oxygen penetration and

465   availability, whereas the decrease was more abrupt at Site 1 within the pockmark. Acoustic

466   evidences of present-day methane outflows reported at this site may also explain the

467   differences in richness patterns between the two sites. This idea comes from the fact that the

468   hydrogen sulfide produced in methane oxidation is toxic for most metazoans (Bagarinao,

1992; Somero et al. 1989), and only well-adapted taxa can tolerate the presence of sulfide compounds, which is usually reflected in low richness (Dando et al., 1991; Diaz and Rosenberg, 1995; Levin, 2005; Levin et al., 2010; Menot et al., 2010; Pearson and Rosenberg, 1978; Sahling et al., 2002; Shirayama and Ohta, 1990; Vanreusel et al., 2010). Regarding macrofauna, Site 1 was characterized by the presence of more tolerant taxa to the pockmark conditions, such as Nemertea, Aplacophora, and Bivalvia, as observed in several cold seeps in northern California, Gulf of Mexico, and New Zealand (Bergquist et al., 2003; Levin, 2000, Levin et al., 2003; Thurber et al., 2013). Other groups, such as Cumacea, Amphipoda, and Isopoda less tolerant to low oxygen availability disappeared inside the pockmark, as observed in other cold-seep sites (Guillon et al., 2017; Levin, 2003; Levin et al., 2010; Menot et al., 2010; Sandulli et al., 2015). The metazoan meiofauna at both sites followed common patterns of communities largely dominated by Nematoda and Copepoda (Giere, 2009; Higgins and Thiel, 1988; Lampadariou et al., 2013; Levin, 2005; Van Gaever et al., 2009a; Zeppilli et al., 2011, 2012, 2018), with Kinorhyncha ranking third in dominance inside the active pockmark (ca. 55 ind/10 cm^2), reaching densities never reported so far from any other deep-sea environment (Neuhaus, 2013). Hyaline and agglutinated foraminifera showed higher abundances inside the pockmark, likely indicating their preference for sediments rich in organic matter content (Fontanier et al., 2018). The picture emerging from these results agrees with the general idea of meiofauna in seepage environment well-adapted to live under these conditions (Bernhard and Sen Gupta, 1999; Duchemin et al., 2007; Duros et al., 2011, Eberwein and Mackensen, 2006; Fontanier et al., 2002, 2008, 2013, 2016; Langezaal et al., 2006; Licari et al., 2003; Vanreusel et al., 2010; Zeppilli et al. 2012).

Our results could also indicate past changes or disturbance events in the pockmark that may have altered the original community (Fontanier et al., 2018). Meiofaunal animals are indeed among the first and the main colonizers of ephemeral and unstable habitats due to their tiny size, rapid generation times, and fast metabolic rates that make them less vulnerable to

496   disturbance than the macrofauna (Giere, 2009; Schratzberger and Ingels, 2018; Woodward,

497   2010). The presence of Kinorhyncha in high abundance (Cepeda et al., 2020) is another

498   unusual feature to support this idea, because they are considered potential colonizers at

499   other sulfidic settings, specifically at deep-sea vents after catastrophic eruptions (Mullineaux

500   et al., 2012); or opportunists in mangrove forests (Ostmann et al., 2012).

501

502   *4.2. Can the dominant taxa function as useful indicators of present and/or past seepage?*

503   In deep-sea seeps, Polychaeta and Nematoda are generally the dominant

504   macrofauna and metazoan meiofauna groups, respectively (Lampadariou et al., 2013; Levin,

505   2005; Menot et al., 2010; Van Gaever et al., 2009a; Zeppilli et al., 2011, 2012, 2018). In this

506   study, only Polychaeta and Nematoda in the uppermost sediment layer followed the general

507   biodiversity patterns found at hypoxic, organically enriched environments, harboring low

508   richness but high abundance (Diaz and Rosenberg, 1995; Pearson and Rosenberg, 1978).

509   Nevertheless only the Nematoda trends proved to be significant and hence effects of the

510   studied pockmark conditions were more evident in this community in the first centimeter of

511   sediment, as considered for this comparison. Considering the whole core, differences in

512   community composition are also significant for Polychaeta (K. Olu, unpubl. data).

513   According to our results, the conditions found in the pockmark likely prevented the survival of

514   some macro- and meiofauna taxa. Within Polychaeta, only Opheliidae were absent in the

515   studied active pockmark, although present in relatively high abundance at Site 2. This family

516   does not seem to tolerate the environmental conditions that characterized the active

517   pockmark area, as inferred from other studies at cold seeps (Guillon et al., 2017; Menot et

518   al., 2010). Similarly, the Nematoda *Pselionema*, *Tricoma,* and *Desmoscolex* usually avoid

519   reduced sediment (Portnova et al., 2014; Zeppilli et al., 2011). This can explain their

520   relatively high densities only at the site away from pockmarks (Site 2), and their presence

521   inside the studied active pockmark as singletons (Site 1). Regarding hyaline foraminifera, *U.*

522   *semiornata* was the only-most abundant species in Site 2, but mostly absent in the

523   pockmark, likely reflecting low tolerance to the environmental constraints.

524   Interestingly, at both studied sites there were several groups known as tolerant of sulfide and

525   hypoxia, such as Spionidae and Syllidae Polychaeta, although not known to dominate

526   polychaete communities at seeps (Gamenick et al., 1998; Guillon et al., 2017; Levin, 2005;

527   Levin et al., 2003, 2006, 2013). Also, other taxa frequently associated with oxygen stress and

528   sediment disturbance, such as the Nematoda genus *Sabatieria* (Garcia et al., 2007; Leduc et

529   al., 2014; Schratzberger et al., 2009), were observed at both sites in low numbers. This

530   fauna, together with the detection of sulfur-bearing minerals at deep layers (black sediment

531   with high amount of pyrite in the pockmark, and detection of free H_2S in very low

532   concentration away from another pockmark field), underline past and present sulfate

533   reduction at both sites. This sulfide production is due to methane diffusion in the pockmark

534   but also because of organoclastic organic matter mineralization without link to fluid or gas

535   emission which is known to have never happened at Site 2 (Pastor et al., 2020).

536   Among the taxa well-adapted to hypoxia and the presence of sulfides (Fauchald and Jumars,

537   1979), four Polychaeta families were exclusive and relatively abundant in the active

538   pockmark: Hesionidae (ca. 25%), Cossuridae (ca. 18%), Polynoidae (ca. 12%), and

539   Capitellidae (ca. 7%). However, only the distribution of Hesionidae was statistically different

540   between the two sites. These four families were often found in sediments enriched in H_2S,

541   methane, organic matter, as well as in oxygen minimum zones, likely indicating tolerance to

542   these hostile conditions (Grassle and Morse-Porteous, 1987; Levin et al., 2003; Menot et al.,

543   2009, 2010; Sahling et al., 2002; Thurber et al., 2013). For instance, Cossuridae are usually

544   abundant at seeps because they appear to feed on anaerobic methane-oxidizing microbes or

545   sulfate-reducing bacteria (Levin et al., 2003; Menot et al., 2010); while Hesionidae,

546   Capitellidae, and Polynoidae are considered opportunist taxa with specific adaptations to

547   hypoxic conditions (Decker et al., 2012; Levin, 2003; Menot et al., 2009, 2010; Ritt et al.,

548   2010). Among the hyaline foraminifera, only one species was absent in Site 2 but relatively

21

abundant in the active pockmark site, *B. alata* (ca. 24%) (reported as well by Fontanier et al., 2016). Regarding the Nematoda community within the studied pockmark, the low genus diversity was attributed to the dominance of a single taxon, *Desmodora*. In fact, this genus was recovered only at this site, accounting for up to 51% of the Nematoda abundance. Comparable Nematoda community composition was reported by Van Gaever et al. (2009b) in cold seeps at the Gulf of Guinea, with low Nematoda richness in the area of seepage influence and with 70% of the abundance belonging to *Sabatieria mortenseni* and *Desmodora* sp. Conversely, surveys on the Mediterranean Sea have revealed higher values of Nematoda richness at pockmarks than at a reference station (Zeppilli et al., 2011), and without dominant taxa in sediments affected by strong gas emissions. Overall only the foraminifer *B. alata*, Hesionidae Polychaeta, and the Nematoda *Desmodora* are typically present in high numbers inside our investigated active pockmark but only *Desmodora* was the best representative of its community at this site.

Some *Desmodora* species were likely not only able to survive under such extreme conditions, but it benefited from pockmark habitat features. In fact, the general Nematoda body shape, long and thin, seems to be an advantage for living in these conditions (Lampadariou et al., 2013). Interestingly, there were epifaunal protists present on several, female specimens of *Desmodora* (16% of the genus abundance; see Annex IV). These protists were loricate ciliates attached along the body surface appearing with no more than four specimens per Nematoda individual. Curiously, similar, attached loricate ciliates were observed on a high number of Kinorhyncha from mangroves (Ostmann et al., 2012), another extreme environment characterized by the presence of dissolved free sulfides in which Kinorhyncha are relatively abundant, as in our study. The conditions generated by sulfides in pockmark and mangrove environments may reduce host fitness and promote epifaunal growth (Hauton et al., 2000; Wang and Chen, 2005). Alternatively, both organisms may draw a mutual advantage from this kind of association in extreme conditions (Baldrighi et al, 2020b).

576

4.3. Inter-community comparison: spatial segregation of benthic components

577

578   Different benthic size components, such as meiofauna and macrofauna, are usually

579   investigated independently even though they are part of the same system in which each

580   component is interconnected. Macro- and meiofauna are biologically linked because several

581   individuals found in the metazoan meiofauna realm are macrofaunal juveniles, the so-called

582   "temporary meiofauna" (Giere, 2009; Higgins and Thiel, 1988). Definitions of macro- and

583   metazoan meiofauna are based on size, specifically on sieve mesh size (Giere, 2009;

584   Higgins and Thiel, 1988; Somerfield and Warwick, 2013), ignoring important ecological traits,

585   as the fact that metazoan meiofauna links macro- and microbenthos. The current definition

586   for separating both communities, albeit short, is supported by recent studies that found

587   macro- and metazoan meiofauna as discrete ecological entities (Somerfield et al., 2018).

588   Our results showed opposite macro- and meiofauna abundance patterns. The study

589   of the benthic fauna along the vertical profiles showed the macrofauna mostly inhabited the

590   uppermost sediment layer (0-1 cm depth) and the metazoan meiofauna was more

591   concentrated at the subsurface layer (1-2 cm depth). Competition for food and other

592   biological interactions (predation) could explain this spatial separation (Van Gaever et al.,

593   2009a). An alternative explanation is that meiofauna, or at least some taxa, are better

594   adapted than macrofauna to the environmental conditions at the subsurface layers, such as

595   high reduced compound concentrations and lower oxygen availability. For instance, as

596   already observed by Fontanier et al. (2016), the high number of foraminifera inside the

597   pockmark was mainly due to *Haplophragmoides bradyi*, *Nouria compressa,* and buliminids,

598   well-adapted taxa to eutrophic environments (Bernhard and Sen Gupta, 1999; Duchemin et

599   al., 2007; Duros et al., 2011, 2013; Eberwein and Mackensen, 2006; Fontanier et al., 2002,

600   2008, 2013; Langezaal et al., 2006; Licari et al., 2003). Hence, under the stressful conditions

601   of the pockmark area, macrofauna are less common and restricted to the well-oxygenated

602　surface sediment layer, whereas metazoan meiofauna and foraminifera exploit this niche,

603　increasing recruitment. Moreover and regarding the low methane emissions in the pockmark,

604　the meiofaunal organisms inhabiting there might be able to survive in the pockmark for a

605　while, preserving the community until the next fluid emission occurs.

606　　　　Finally, the original meiofauna community may also have been affected by

607　disturbance events in the pockmark, i.e. an increase of sedimentation from terrestrial origin

608　(Fontanier et al., 2018), altering density and composition. Meiofaunal animals are among the

609　first and the main colonizers of ephemeral and unstable habitats, because their biological

610　features make them less vulnerable to disturbance than macrofauna (Giere, 2009;

611　Schratzberger and Ingels, 2018; Woodward, 2010). Accordingly, we observed elevated

612　Kinorhyncha density (discussed above, see section 5.1) and the presence of some

613　Nematoda genera, such as *Sabatieria*, often recovered at disturbed sediments (Garcia et al.,

614　2007; Leduc et al., 2014; Schratzberger et al., 2009). Similarly, the relatively higher

615　abundance inside the pockmark of the foram *B. marginata* suggested a recent disturbance

616　event, because it generally appeared in unstable and ephemeral cold seeps acting as

617　pioneer species (Fontanier et al., 2014a; 2014b; 2016; Hess et al., 2005; Hess and Jorissen,

618　2009).

619

620　**5. Conclusions**

621　The present study investigated the distribution and diversity of benthic communities from a

622　pockmark environment by using a threefold approach and the effect of environmental

623　conditions on different infauna components. Despite the reduced number of sampling sites,

624　we could make the following conclusions with caution in data interpretation:

625　1) At the studied active pockmark, macro-, metazoan meiofauna and foraminiferans showed

626　differences in their taxonomic composition compared to fauna found at a site located away

627　from another pockmark field. Macrofauna showed lower abundance and lower diversity with

24

628   dominance of well-adapted taxa, while the higher meiofaunal abundances reflected the

629   presence of taxa able to take advantage of the environmental constraints. Environmental

630   features that characterized the two study sites likely played a key role in determining the

631   variation of infauna at both sites and along the vertical profile in terms of number of taxa,

632   abundance and community composition, possibly due to geochemical and biological

633   conditions induced by organic matter degradation and oxidation of methane process along

634   with lower oxygen availability in the pockmark.

635   2) Macrofauna were more abundant in layers harboring low metazoan meiofaunal densities

636   (0-1 cm depth), that corresponded to well-oxygenated layers. Differently, specific meiofaunal

637   taxa can tolerate low oxygen levels and seems more competitive under these conditions.

638   3) Considering the dominant taxa, Polychaeta and Nematoda followed the general trends

639   usually reported in extreme environments, with low diversity and high abundance. In the

640   active pockmark, Polychaeta were characterized by a dominance of families adapted to

641   sulfide-rich and oxygen-depleted environments. High abundance of the foraminifer *Bulimina*

642   *marginata* was also indicative of a disturbance event, associated with either methane flux or

643   organic matter inputs. Similarly, most of the Nematoda abundance was due to *Desmodora*.

644   Thus, the *Desmodora* genus could then be a potential benthic candidate indicator of stressed

645   environmental conditions related to fluid emissions, but further studies at the area testing this

646   are needed.

647   4) The detection of dissolved free sulfide in low concentrations away from the pockmark

648   area, along with the presence of some organisms able to tolerate sulfide-rich and/or hypoxic

649   conditions indicate that this off-site may be an ecotone in which the sulfide concentrations

650   are not selective for most of the heterotrophic organisms, allowing their co-occurrence with

651   fauna associated with reduced environments.

652

653   **6. Acknowledgments**

25

665 **Author contribution:** KO and SD conceived and designed the sampling strategy; NS wrote

666 the first draft of the manuscript, analyzed the data; KO, AV and DZ conceived the analytical

667 methods for macrofauna and meiofauna respectively; EB identified the Nematoda

668 specimens; MGL processed the macrofauna data; LM processed meiofauna on board; CB

669 and LP provided geochemical data; SD was involved in the water column acoustic data

670 acquisition, processing and interpretation; GG helped with the data analyses; all authors

671 helped revise the manuscript, and read and approved the revised version.

672 **References**

673 Bagarinao, T., 1992. Sulfide as an environmental factor and toxicant: tolerance and
674   adaptations in aquatic organisms. Aquat. Toxicol. 24, 21–62.
675   https://doi.org/10.1016/0166-445X(92)90015-F
676 Baldrighi, E., Zeppilli, D., Appolloni, L., Donnarumma, L., Chianese, E., Russo, G.F.,
677   Sandulli, R., 2020(a). Meiofaunal communities and nematode diversity characterizing
678   the Secca delle Fumose shallow vent area (Gulf of Naples, Italy). PeerJ 8:e9058 DOI
679   10.7717/peerj.9058
680 Elisa Baldrighi, E., Dovgal, I., Zeppilli, D., Abibulaeva. A., Michelet, C., Michaud, E., Franzo,
681   A., Grassi, E., Cesaroni, L., Guidi, L., Balsamo, M., Sandulli, R., Semprucci, F.,
682   2020(b). The Cost for Biodiversity: Records of Ciliate-Nematode Epibiosis with the
683   Description of Three New Suctorian Species. Diversity, 12(6), 224;
684   https://doi.org/10.3390/d12060224 - 04
685 Bergquist, D.C., Ward, T., Cordes, E.E., McNelis, T., Howlett, S., Koisoff, R., Hourdez, S.,
686   Carney, R. & Fisher, C.R., 2003. Community structure of vestimentiferan-generated
687   habitat islands from Gulf of Mexico cold seeps. J. Exp. Mar. Biol. Ecol. 289, 197–222.
688 Bernhard, J.M., Sen Gupta, B.K., 1999. Foraminifera of oxygen-depleted environments, in:
689   Modern Foraminifera. Springer Netherlands, Dordrecht, pp. 201–216.
690   https://doi.org/10.1007/0-306-48104-9_12
691 Cepeda, D., Pardos, F., Zeppilli, D., Sánchez, N., 2020. Dragons of the Deep Sea:
692   Kinorhyncha Communities in a Pockmark Field at Mozambique Channel, With the
693   Description of Three New Species. Frontiers in Mar. Sci. 7, 665;
694   https://www.frontiersin.org/article/10.3389/fmars.2020.00665
695 Cline, J.D., 1969. Spectrophotometric determination of hydrogen sulfide in natural
696   waters. Limnol. Oceanogr. 14(3), 454–458. https://doi.org/10.4319/lo.1969.14.3.0454
697 Crawley, M.J., 2012. The R Book: Crawley/The R Book. John Wiley & Sons, Ltd, Chichester,
698   UK. https://doi.org/10.1002/9781118448908
699 Dando, P.R., Austen, M.C., Burke, R.A., Kendall, M.A., Kennicutt, M.C., Judd, A.G., Moore,
700   D.C., O'Hara, S.C.M., Schmalijohann, R., Southward, A.J., 1991. Ecology of a North
701   Sea pockmark with an active methane seep. Mar. Ecol. Prog. Ser. 70, 49–63.
702 Danovaro, R., 2010. Methods for the Study of Deep-Sea Sediments, Their Functioning and
703   Biodiversity. https://doi.org/10.1201/9781439811382
704 Decker, C., Morineaux, M., Van Gaever, S., Caprais, J.-C., Lichtschlag, A., Gauthier, O.,
705   Andersen, A.C., Olu, K., 2012. Habitat heterogeneity influences cold-seep
706   macrofaunal communities within and among seeps along the Norwegian margin. Part
707   1: macrofaunal community structure. Mar. Ecol.- Evol. Perspect. 33, 205–230.
708   https://doi.org/10.1111/j.1439-0485.2011.00503.x
709 Diaz, R.J., Rosenberg, R., 1995. Marine benthic hypoxia: a review of its ecological effects
710   and the behavioural responses of benthic macrofauna. Oceanogr. Mar. Biol. Annu.
711   Rev.
712 Donnarumma, L., Appolloni, L., Chianese, E., Bruno, R., Baldrighi, E., Guglielmo, R., Russo,
713   G.F., Zeppilli, D., Sandulli, R, 2019. Environmental and benthic community patterns of
714   the shallow hydrothermal area of Secca Delle Fumose (Baia, Naples,Italy). Front.
715   Mar. Sci. 6:685. doi: 10.3389/fmars.2019.00685
716 Duchemin, G., Fontanier, C., Jorissen, F.J., Barras, C., Griveaud, C., 2007. Living small-
717   sized (63–150 μm) foraminifera from mid-shelf to mid-slope environments in the Bay
718   of Biscay. J. Foraminifer. Res. 37, 12–32. https://doi.org/10.2113/gsjfr.37.1.12
719 Dupré, S., Battani, A., Deville, E., Scalabrin, C., Olu, K., Poort, J., Bermell, S., Dupont, P.,
720   Gaillot, A., Guérin, C., Pierre, D., Ogor, A., Théréau, E., Thomas, Y., Jouët, G., and
721   Jorry, S., 2019. Focused fluid flows and seeps offshore southern Majunga Basin (NW
722   Madagascar), AGU Fall Meeting: San Francisco, USA, p. 515706

Dupré S, Scalabrin C, Grall C, Augustin AH, Henry P, Şengör AMC, Görür N, Çağatay N, Géli L (2015) Tectonic and sedimentary controls for widespread gas emissions in the Sea of Marmara. Results from systematic, shipborne multibeam echosounder water column imageries. Journal of Geophysical Research 120 (5):2891-2912. doi:10.1002/2014JB011617

Duros, P., Fontanier, C., Metzger, E., Cesbron, F., Deflandre, B., Schmidt, S., Buscail, R., Zaragosi, S., Kerhervé, P., Rigaud, S., Delgard, M.-L., Jorissen, F.J., 2013. Live (stained) benthic foraminifera from the Cap-Ferret Canyon (Bay of Biscay, NE Atlantic): A comparison between the canyon axis and the surrounding areas. Deep Sea Res. Part Oceanogr. Res. Pap. 74, 98–114. https://doi.org/10.1016/j.dsr.2013.01.004

Duros, P., Fontanier, C., Metzger, E., Pusceddu, A., Cesbron, F., de Stigter, H.C., Bianchelli, S., Danovaro, R., Jorissen, F.J., 2011. Live (stained) benthic foraminifera in the Whittard Canyon, Celtic margin (NE Atlantic). Deep Sea Res. Part Oceanogr. Res. Pap. 58, 128–146. https://doi.org/10.1016/j.dsr.2010.11.008

Eberwein, A., Mackensen, A., 2006. Regional primary productivity differences off Morocco (NW-Africa) recorded by modern benthic foraminifera and their stable carbon isotopic composition. Deep Sea Res. Part Oceanogr. Res. Pap. 53, 1379–1405. https://doi.org/10.1016/j.dsr.2006.04.001

Fauchald, K., Jumars, P.A., 1979. Diet of worms: a study of polychaete feeding guilds. Ocean. Mar Biol U. S. 17.

Fontanier, C., Duros, P., Toyofuku, T., Oguri, K., Koho, K.A., Buscail, R., Grémare, A., Radakovitch, O., Deflandre, B., Nooijer, L.J.D., Bichon, S., Goubet, S., Ivanovsky, A., Chabaud, G., Menniti, C., Reichart, G.-J., Kitazato, H., 2014(a). Living (stained) deep-sea foraminifera off Hachinohe (NE japan, Western pacific): environmental interplay in oxygen-depleted ecosystems. J. Foraminifer. Res. 44, 281–299. https://doi.org/10.2113/gsjfr.44.3.281

Fontanier, C., Garnier, E., Brandily, C., Dennielou, B., Bichon, S., Gayet, N., Eugene, T., Rovere, M., Grémare, A., Deflandre, B., 2016. Living (stained) benthic foraminifera from the Mozambique Channel (eastern Africa): Exploring ecology of deep-sea unicellular meiofauna. Deep Sea Res. Part Oceanogr. Res. Pap. 115, 159–174. https://doi.org/10.1016/j.dsr.2016.06.007

Fontanier, C., Jorissen, F., Geslin, E., Zaragosi, S., Duchemin, G., Laversin, M., Gaultier, M., 2008. Live and dead foraminiferal faunas from Saint-Tropez canyon (Bay of Frejus): observations based on in situ and incubated cores. J. Foraminifer. Res. 38, 137–156. https://doi.org/10.2113/gsjfr.38.2.137

Fontanier, C., Jorissen, F.J., Licari, L., Alexandre, A., Anschutz, P., Carbonel, P., 2002. Live benthic foraminiferal faunas from the Bay of Biscay: faunal density, composition, and microhabitats. Deep Sea Res. Part Oceanogr. Res. Pap. 49, 751–785. https://doi.org/10.1016/S0967-0637(01)00078-4

Fontanier, C., Koho, K.A., Goñi-Urriza, M.S., Deflandre, B., Galaup, S., Ivanovsky, A., Gayet, N., Dennielou, B., Grémare, A., Bichon, S., Gassie, C., Anschutz, P., Duran, R., Reichart, G.J., 2014(b). Benthic foraminifera from the deep-water Niger delta (Gulf of Guinea): Assessing present-day and past activity of hydrate pockmarks. Deep Sea Res. Part Oceanogr. Res. Pap. 94, 87–106. https://doi.org/10.1016/j.dsr.2014.08.011

Fontanier, C., Mamo, B., Toucanne, S., Bayon, G., Schmidt, S., Deflandre, B., Dennielou, B., Jouet, G., Garnier, E., Sakai, S., Lamas, R.M., Duros, P., Toyofuku, T., Salé, A., Belleney, D., Bichon, S., Boissier, A., Chéron, S., Pitel, M., Roubi, A., Rovere, M., Grémare, A., Dupré, S., Jorry, S.J., 2018. Are deep-sea ecosystems surrounding Madagascar threatened by land-use or climate change? Deep Sea Res. Part Oceanogr. Res. Pap. 131, 93–100. https://doi.org/10.1016/j.dsr.2017.11.011

Fontanier, C., Metzger, E., Waelbroeck, C., Jouffreau, Mé., LeFloch, N., Jorissen, F., Etcheber, H., Bichon, S., Chabaud, G., Poirier, D., Grémare, A., Deflandre, B., 2013. Live (Stained) Benthic Foraminifera Off Walvis Bay, Namibia: A Deep-Sea Ecosystem

777   under the Influence of Bottom Nepheloid Layers. J. Foraminifer. Res. 43, 55–71.
778   https://doi.org/10.2113/gsjfr.43.1.55
779 Gamenick, I., Vismann, B., Grieshaber, M.K., Giere, O.W., 1998. Ecophysiological
780   differentiation of Capitella capitata (Polychaeta). Sibling species from different sulfidic
781   habitats. https://doi.org/10.3354/meps175155
782 Garcia, R., Koho, K., De Stigter, H., Epping, E., Koning, E., Thomsen, L., 2007. Distribution
783   of meiobenthos in the Nazaré canyon and adjacent slope (western Iberian Margin) in
784   relation to sedimentary composition. Mar. Ecol. Prog. Ser. 340, 207–220.
785   https://doi.org/10.3354/meps340207
786 Giere, O., 2009. Meiobenthology: The Microscopic Motile Fauna of Aquatic Sediments, 2nd
787   ed. Springer-Verlag, Berlin Heidelberg.
788 Gooday, A.J., Levin, L.A., Aranda da Silva, A., Bett, B.J., Cowie, G.L., Dissard, D., Gage,
789   J.D., Hughes, D.J., Jeffreys, R., Lamont, P.A., Larkin, K.E., Murty, S.J., Schumacher,
790   S., Whitcraft, C., Woulds, C., 2009. Faunal responses to oxygen gradients on the
791   Pakistan margin: A comparison of foraminiferans, macrofauna and megafauna. Deep
792   Sea Res. Part II Top. Stud. Oceanogr., Benthic Biological and Biogeochemical
793   Patterns and Processes Across an Oxygen Minimum Zone (Pakistan Margin, NE
794   Arabian Sea) 56, 488–502. https://doi.org/10.1016/j.dsr2.2008.10.003
795 Grasshoff, K., Kremling, K., Ehrhardt, M. (eds.), 1999. Methods of Seawater Analysis. 3rd
796   edition. Weinheim: Wiley-VCH. 632 pages.
797 Grassle, J.F., Morse-Porteous, L.S., 1987. Macrofaunal colonization of disturbed deep-sea
798   environments and the structure of deep-sea benthic communities. Deep Sea Res.
799   Part Oceanogr. Res. Pap. 34, 1911–1950. https://doi.org/10.1016/0198-
800   0149(87)90091-4
801 Guillon, E., Menot, L., Decker, C., Krylova, E., Olu, K., 2017. The vesicomyid bivalve habitat
802   at cold seeps supports heterogeneous and dynamic macrofaunal assemblages. Deep
803   Sea Res. Part Oceanogr. Res. Pap. 120, 1–13.
804   https://doi.org/10.1016/j.dsr.2016.12.008
805 Hauton, C., Hawkins, L.E., Hutchinson, S., 2000. The effects of salinity on the interaction
806   between a pathogen (Listonella anguillarum) and components of a host (Ostrea
807   edulis) immune system. Comp. Biochem. Physiol. B Biochem. Mol. Biol. 127, 203–
808   212. https://doi.org/10.1016/S0305-0491(00)00251-0
809 Heip, C., Vincx, M., Vranken, G., 1985. The ecology of marine nematodes.
810 Hess, S., Jorissen, F.J., 2009. Distribution patterns of living benthic foraminifera from Cap
811   Breton canyon, Bay of Biscay: Faunal response to sediment instability. Deep Sea
812   Res. Part Oceanogr. Res. Pap. 56, 1555–1578.
813   https://doi.org/10.1016/j.dsr.2009.04.003
814 Hess, S., Jorissen, F.J., Venet, V., Abu-Zied, R., 2005. Benthic foraminiferal recovery after
815   recent turbidite deposition in Cap breton canyon, Bay of Biscay. J. Foraminifer. Res.
816   35, 114–129. https://doi.org/10.2113/35.2.114
817 Hessler, R.R., Jumars, P.A., 1974. Abyssal community analysis from replicate box cores in
818   the central North Pacific. Suppl. Hessler RR Jumars PA 1974 Abyssal Community
819   Anal. Replicate Cores Cent. North Pac. Deep Sea Res. Oceanogr. Abstr. 213 185-
820   209 Httpsdoiorg1010160011-74717490058-8.
821   https://doi.org/10.1594/PANGAEA.692265
822 Higgins, R.P., Thiel, H., 1988. Introduction to the study of meiofauna. Washington, D.C. :
823   Smithsonian Institution Press.
824 Hovland, M., Judd, A.G., 1988. Seabed pockmarks and seepages: impact on geology,
825   biology and marine environment. Grahamand Trotman, London.
826 Jensen, P., 1986. Nematode fauna in the sulphide-rich brine seep and adjacent bottoms of
827   the East Flower Garden, NW Gulf of Mexico. Mar. Biol. 92, 489–503.
828   https://doi.org/10.1007/BF00392509
829 Jorry, S.J., 2014. ⟨http://dx.doi.org/10.17600/14000900⟩.
830 Lampadariou, N., Kalogeropoulou, V., Sevastou, K., Keklikoglou, K., Sarrazin, J., 2013.
831   Influence of chemosynthetic ecosystems on nematode community structure and

832   biomass in the deep eastern Mediterranean Sea. Biogeosciences 10, 5381–5398.
833   https://doi.org/10.5194/bg-10-5381-2013
834 Langezaal, A.M., Jorissen, F.J., Braun, B., Chaillou, G., Fontanier, C., Anschutz, P., van der
835   Zwaan, G.J., 2006. The influence of seasonal processes on geochemical profiles and
836   foraminiferal assemblages on the outer shelf of the Bay of Biscay. Cont. Shelf Res.
837   26, 1730–1755. https://doi.org/10.1016/j.csr.2006.05.005
838 Leduc, D., Rowden, A.A., Nodder, S.D., Berkenbusch, K., Probert, P.K., Hadfield, M.G.,
839   2014. Unusually high food availability in Kaikoura Canyon linked to distinct deep-sea
840   nematode community. Deep Sea Res. Part II Top. Stud. Oceanogr., Submarine
841   Canyons: Complex Deep-Sea Environments Unravelled by Multidisciplinary Research
842   104, 310–318. https://doi.org/10.1016/j.dsr2.2013.06.003
843 Legendre, P., Gallagher, E.D., 2001. Ecologically meaningful transformations for ordination
844   of species data. Oecologia 129, 271–280. https://doi.org/10.1007/s004420100716
845 Levin, L.A., 2003. Oxygen minimum zone benthos: Adaptation and community response to
846   hypoxia. Oceanogr. Mar. Biol. Vol 41 41, 1–45.
847 Levin, L.A., 2000. Do methane seeps support distinct macrofaunal assemblages?
848   Observations on community structure and nutrition from the northern California slope
849   and shelf. Mar. Ecol.-Prog. Ser. 208, 21–39. https://doi.org/10.3354/meps208021
850 Levin, L.A., Ziebis, W., Mendoza, G., Bertics, V., Washington, T., Gonzalez, J., Thurber,
851   A.R., Ebbed, B., Lee, R., 2013. Ecological release and niche partitioning under stress:
852   Lessons from dorvilleid polychaetes in sulfidic sediments at methane seeps. Deep-
853   Sea Res. Part Ii-Top. Stud. Oceanogr. 92, 214–233.
854   https://doi.org/10.1016/j.dsr2.2013.02.006
855 Levin, L.A., 2005. Ecology of cold seep sediments: interactions of fauna with flow, chemistry
856   and microbes. https://doi.org/10.1201/9781420037449-3
857 Levin, L.A., Huggett, C.L., Wishner, K.F., 1991. Control of deep-sea benthic community
858   structure by oxygen and organic-matter gradients in the eastern Pacific Ocean. J.
859   Mar. Res. 49, 763–800. https://doi.org/10.1357/002224091784995756
860 Levin, L.A., Mendoza, G.F., Gonzalez, J.P., Thurber, A.R., Cordes, E.E., 2010. Diversity of
861   bathyal macrofauna on the northeastern Pacific margin: the influence of methane
862   seeps and oxygen minimum zones. Mar. Ecol. 31, 94–110.
863   https://doi.org/10.1111/j.1439-0485.2009.00335.x
864 Levin, L.A., Sibuet, M., 2012. Understanding continental margin biodiversity: a new
865   imperative. Annu. Rev. Mar. Sci. 4, 79–112. https://doi.org/10.1146/annurev-marine-
866   120709-142714
867 Levin, L.A., Ziebis, W., Mendoza, G.F., Growney, V.A., Tryon, M.D., Brown, K.M., Mahn, C.,
868   Gieskes, J.M., Rathburn, A.E., 2003. Spatial heterogeneity of macrofauna at northern
869   California methane seeps:: influence of sulfide concentration and fluid flow. Mar. Ecol.
870   Prog. Ser. 265, 123–139.
871 Levin, L.A., Ziebis, W., Mendoza, G.F., Growney-Cannon, V., Walther, S., 2006. Recruitment
872   response of methane-seep macrofauna to sulfide-rich sediments: An in situ
873   experiment. J. Exp. Mar. Biol. Ecol., A Tribute to Richard M. Warwick 330, 132–150.
874   https://doi.org/10.1016/j.jembe.2005.12.022
875 Licari, L.N., Schumacher, S., Wenzhöfer, F., Zabel, M., Mackensen, A., 2003. Communities
876   and microhabitats of living benthic foraminifera from the tropical east Atlantic: impact
877   of different productivity regimes. J. Foraminifer. Res. 33, 10–31.
878   https://doi.org/10.2113/0330010
879 Menot, L., Crassous, P., Desbruyères, D., Galéron, J., Khripounoff, A., Sibuet, M., 2009.
880   Colonization patterns along the equatorial West African margin: Implications for
881   functioning and diversity maintenance of bathyal and abyssal communities. Deep Sea
882   Res. Part II Top. Stud. Oceanogr., Deep-Sea Benthic Ecosystems of the Equatorial
883   African Margin: The Multidisciplinary BIOZAIRE Program 56, 2313–2325.
884   https://doi.org/10.1016/j.dsr2.2009.04.012
885 Menot, L., Sibuet, M., Carney, R.S., Levin, L.A., Rowe, G.T., Billett, D.S.M., Poore, G.,
886   Kitazato, H., Vanreusel, A., Galéron, J., Lavrado, H.P., Sellanes, J., Ingole, B.,

887   Krylova, E., 2010. New Perceptions of Continental Margin Biodiversity, in: Life in the
888   World's Oceans. John Wiley & Sons, Ltd, pp. 79–102.
889   https://doi.org/10.1002/9781444325508.ch5
890   Montagna, P.A., Baguley, J.G., Hsiang, C.Y. and Reuscher, M.G. (2017), Comparison of
891   sampling methods for deep-sea infauna. Limnol. Oceanogr. Methods. 15, 166-183.
892   doi:10.1002/lom3.10150
893   Montagna, P.A., Bauer, J.E., Hardin, D., Spies, R.B., 1989. Vertical distribution of microbial
894   and meiofaunal populations in sediments of a natural coastal hydrocarbon seep. J.
895   Mar. Res. 47, 657–680. https://doi.org/10.1357/002224089785076226
896   Mullineaux, L.S., Bris, N.L., Mills, S.W., Henri, P., Bayer, S.R., Secrist, R.G., Siu, N., 2012.
897   Detecting the Influence of Initial Pioneers on Succession at Deep-Sea Vents. PLOS
898   ONE 7, e50015. https://doi.org/10.1371/journal.pone.0050015
899   Neuhaus, B., 2013. Kinorhyncha (= Echinodera). Handb. Zool. 2010.
900   Oksanen, J., Blanchet, F.G., Kindt, R., Legendre, P., Minchin, P.R., O'Hara, R.B., Simpson,
901   G.L., Solymos, P., Stevens, M.H.H, Wagner, H., 2015. Vegan: community ecology
902   package. R package vegan, vers. 2.2-1.
903   Oksanen, J., Blanchet, F.G., Friendly, M., Kindt, R., Legendre, P., McGlinn, D., Minchin,
904   P.R., O'Hara, R.B., Simpson, G.L., Solymos, P., Stevens, M.H.H., Eduard, S.E.,
905   Wagner, H., 2018. Vegan: Community Ecology Package. R package version 2.5-2.
906   https://CRAN.R-project.org/ package=vegan.
907   Olu, K., 2014. PAMELA-MOZ01 cruise,L'Atalante R/V. https://doi.org/10.17600/14001000
908   Ostmann, A., Nordhaus, I., Sørensen, M.V., 2012. First recording of kinorhynchs from Java,
909   with the description of a new brackish water species from a mangrove-fringed lagoon.
910   Mar. Biodivers. 42, 79–91. https://doi.org/10.1007/s12526-011-0094-z
911   Pastor, L., Brandily, C., Schmidt, S., Miramontes, E., Péron, M., Apperé, D., Besson, S.,
912   Boissier, A., Jouet, G., 2020. Modern sedimentation and geochemical imprints in
913   sediments from the NW Madagascar margin. Mar. Geol. 426.
914   https://doi.org/10.1016/j.margeo.2020.106184
915   Pastor, L., Deflandre, B., Viollier, E., Cathalot, C., Metzger, E., Rabouille, C., Escoubeyrou,
916   K., Lloret, E., Pruski, A., Vétion, G., Desmalades, M., Buscail, R., Grémare, A.,
917   2011. Influence of the organic matter composition on benthic oxygen demand in the
918   Rhône prodelta (NW Mediterranean Sea). Continental Shelf Research. 31(9), 1008–
919   1019.
920   Pearson, T.H., Rosenberg, R., 1978. Macrobenthic succession in relation to organic
921   enrichment and pollution of the marine environment. Ocean. Mar Biol Ann Rev 16,
922   229–311.
923   Portail, M., Olu, K., Escobar-Briones, E., Caprais, J.C., Menot, L., Waeles, M., Cruaud, P.,
924   Sarradin, P.M., Godfroy, A., Sarrazin, J., 2015. Comparative study of vent and seep
925   macrofaunal communities in the Guaymas Basin. Biogeosciences 12, 5455–5479.
926   https://doi.org/10.5194/bg-12-5455-2015
927   Portnova, D.A., Mokievsky, V.O., Haflidason, H., Todt, K., 2014. Metazoan meiobenthos and
928   nematode assemblages in the Nyegga Region of methane seepage (Norwegian Sea).
929   Russ. J. Mar. Biol. 40, 255–265. https://doi.org/10.1134/S1063074014040075
930   Powell, E.N., Bright, T.J., Woods, A., Gittings, S., 1983. Meiofauna and the thiobios in the
931   East Flower Garden Brine Seep. Mar. Biol.,73, 269–283.
932   Ritt, B., Pierre, C., Gauthier, O., Wenzhöfer, F., Boetius, A., Sarrazin, J., 2011. Diversity and
933   distribution of cold-seep fauna associated with different geological and environmental
934   settings at mud volcanoes and pockmarks of the Nile Deep-Sea Fan. Mar. Biol. 158,
935   1187–1210. https://doi.org/10.1007/s00227-011-1679-6
936   Ritt, B., Sarrazin, J., Caprais, J.-C., Noël, P., Gauthier, O., Pierre, C., Henry, P.,
937   Desbruyères, D., 2010. First insights into the structure and environmental setting of
938   cold-seep communities in the Marmara Sea. Deep Sea Res. Part Oceanogr. Res.
939   Pap. 57, 1120–1136. https://doi.org/10.1016/j.dsr.2010.05.011
940   Rouse, G., Pleijel, F., 2001. Polychaetes. Oxford University Press, Oxford, New York.

941 Rouse, G., Fauchald, K., 1997. Cladistics and polychaetes. Zool. Scr. 26, 139–204.
942 https://doi.org/10.1111/j.1463-6409.1997.tb00412.x
943 Sahling, H., Rickert, D., Lee, R.W., Linke, P., Suess, E., 2002. Macrofaunal community
944 structure and sulfide flux at gas hydrate deposits from the Cascadia convergent
945 margin, NE Pacific. Mar. Ecol. Prog. Ser. 231, 121–138.
946 https://doi.org/10.3354/meps231121
947 Sandulli, R., Miljutin, D., Angeletti, L. and Taviani, M., 2015. Meiobenthos and nematode
948 assemblages from different deep-sea habitats of the Strait of Sicily (Central
949 Mediterranean Sea). Medit. Mar. Sci. 16 (2), 402-412.
950 http://dx.doi.org/10.12681/mms.1145
951 Schratzberger, M., Ingels, J., 2018. Meiofauna matters: The roles of meiofauna in
952 benthic ecosystems. J. Exp. Mar. Biol. Ecol. 502, 12–25.
953 Schratzberger, M., Lampadariou, N., Somerfield, P.J., Vandepitte, L., Vanden Berghe, E.,
954 2009. The impact of seabed disturbance on nematode communities: linking field and
955 laboratory observations. Mar. Biol. 156, 709–724. https://doi.org/10.1007/s00227-008-
956 1122-9
957 Shirayama, Y., Ohta, S., 1990. Meiofauna in a cold-seep community off Hatsushima, central
958 Japan. J. Oceanogr. Soc. Jpn. 46, 118–124. https://doi.org/10.1007/BF02123438
959 Sibuet, M., Olu, K., 1998. Biogeography, biodiversity and fluid dependence of deep-sea cold-
960 seep communities at active and passive margins. Deep Sea Res. Part II Top. Stud.
961 Oceanogr. 45, 517–567. https://doi.org/10.1016/S0967-0645(97)00074-X
962 Somerfield, P.J., Dashfield, S.L., Warwick, R.M., 2018. The structure and organisation of
963 integral marine benthic communities in relation to sieve mesh size. J. Exp. Mar. Biol.
964 Ecol., IçIMCo, the 16th International Meiofauna Conference 502, 164–173.
965 https://doi.org/10.1016/j.jembe.2017.08.007
966 Somerfield, P.J., Warwick, R.M., 2013. Meiofauna Techniques, in: Methods for the Study of
967 Marine Benthos. John Wiley & Sons, Ltd, pp. 253–284.
968 https://doi.org/10.1002/9781118542392.ch6
969 Somero, G.N., Childress, J.J., Anderson, A.E., 1989. Transport, metabolism, and
970 detoxification of hydrogen sulfide in animals from sulfide-rich marine environments.
971 Aquat. Sci., 1, 591–614.
972 Thurber, A.R., Levin, L.A., Rowden, A.A., Sommer, S., Linke, P., Kröger, K., 2013. Microbes,
973 macrofauna, and methane: A novel seep community fueled by aerobic
974 methanotrophy. Limnol. Oceanogr. 58, 1640–1656.
975 https://doi.org/10.4319/lo.2013.58.5.1640
976 Van Gaever, S., Galerón, J., Sibuet, M., Vanreusel, A., 2009b. Deep-sea habitat
977 heterogeneity influence on meiofaunal communities in the Gulf of Guinea. Deep Sea
978 Res. Part Oceanogr. Res. Pap. 56, 2259–2269.
979 Van Gaever, S., Moodley, L., de Beer, D., Vanreusel, A., 2006. Meiobenthos at the Arctic
980 Håkon Mosby Mud Volcano, with a parental-caring nematode thriving in sulphide-rich
981 sediments. Mar. Ecol.-Prog. Ser. 321, 143–155.
982 http://dx.doi.org/10.3354/meps321143
983 Van Gaever, S., Olu, K., Derycke, S., Vanreusel, A., 2009a. Metazoan meiofaunal
984 communities at cold seeps along the Norwegian margin: Influence of habitat
985 heterogeneity and evidence for connection with shallow-water habitats. Deep Sea
986 Res. Part Oceanogr. Res. Pap. 56, 772–785.
987 https://doi.org/10.1016/j.dsr.2008.12.015
988 Vanreusel, A., De Groote, A., Gollner, S., Bright, M., 2010. Ecology and biogeography of
989 free-living nematodes associated with chemosynthetic environments in the deep sea:
990 a review. PloS One 5, e12449. https://doi.org/10.1371/journal.pone.0012449
991 Wang, L.-U., Chen, J.-C., 2005. The immune response of white shrimp Litopenaeus
992 vannamei and its susceptibility to Vibrio alginolyticus at different salinity levels. Fish
993 Shellfish Immunol. 18, 269–278. https://doi.org/10.1016/j.fsi.2004.07.008
994 Woodward, 2010. Integrative Ecology. Elsevier Science.

995   Zeppilli, D., Canals, M., Danovaro, R., 2012. Pockmarks enhance deep-sea benthic
996   biodiversity: a case study in the western Mediterranean Sea. Divers. Distrib. 18, 832–
997   846. https://doi.org/10.1111/j.1472-4642.2011.00859.x
998   Zeppilli, D., Leduc, D., Fontanier, C., Fontaneto, D., Fuchs, S., Gooday, A.J., Goineau, A.,
999   Ingels, J., Ivanenko, V.N., Kristensen, R.M., Neves, R.C., Sanchez, N., Sandulli, R.,
1000   Sarrazin, J., Sørensen, M.V., Tasiemski, A., Vanreusel, A., Autret, M., Bourdonnay,
1001   L., Claireaux, M., Coquillé, V., De Wever, L., Rachel, D., Marchant, J., Toomey, L.,
1002   Fernandes, D., 2018. Characteristics of meiofauna in extreme marine ecosystems: a
1003   review. Mar. Biodivers. 48, 35–71. https://doi.org/10.1007/s12526-017-0815-z
1004   Zeppilli, D., Mea, M., Corinaldesi, C., Danovaro, R., 2011. Mud volcanoes in the
1005   Mediterranean Sea are hot spots of exclusive meiobenthic species. Prog. Oceanogr.
1006   91, 260–272. https://doi.org/10.1016/j.pocean.2011.01.001
1007   Zeppilli, D., Sarrazin, J., Leduc, D., Arbizu, P.M., Fontaneto, D., Fontanier, C., Gooday, A.J.,
1008   Kristensen, R.M., Ivanenko, V.N., Sørensen, M.V., Vanreusel, A., Thébault, J., Mea,
1009   M., Allio, N., Andro, T., Arvigo, A., Castrec, J., Danielo, M., Foulon, V., Fumeron, R.,
1010   Hermabessiere, L., Hulot, V., James, T., Langonne-Augen, R., Le Bot, T., Long, M.,
1011   Mahabror, D., Morel, Q., Pantalos, M., Pouplard, E., Raimondeau, L., Rio-Cabello, A.,
1012   Seite, S., Traisnel, G., Urvoy, K., Van Der Stegen, T., Weyand, M., Fernandes, D.,
1013   2015. Is the meiofauna a good indicator for climate change and anthropogenic
1014   impacts? Mar. Biodivers. 45, 505–535. https://doi.org/10.1007/s12526-015-0359-z
1015   Zuur, A., Ieno, E.N., Smith, G.M., 2007. Analyzing Ecological Data, Statistics for Biology and
1016   Health. Springer-Verlag, New York.
1017

Figure captions

1019 Fig. 1 a) Relief map (from Globe software © Ifremer) with location of the study sites offshore
1020 northwestern Madagascar margin in the Mozambique Channel. The Blue Marble data (2004)
1021 is courtesy of Reto Stockli (NASA/GSFC). b) Shaded bathymetry map offshore Majunga
1022 Basin (northwestern Madagascar margin) from the PTOLEMEE and PAMELA-MOZ01
1023 oceanographic expeditions with locations of the two sampling sites. c) 2D water column polar
1024 echogram and seafloor shaded bathymetry in the pockmark area of Site 1. Acoustic anomaly
1025 in the water column is interpreted as gas bubbles escaping from the seafloor at this location.
1026 d) Detailed bathymetry of the active pockmark Site 1 showing the SCAMPI immersion path
1027 and location of the sampling sites. e) Detailed bathymetry of the Site 2, away from a
1028 pockmark field, showing the SCAMPI immersion path and location of the sampling sites.

1029 Fig. 2 Faunal community structure characterizing the study sites. Faunal composition of each
1030 site is given according to studied layers along the vertical profile of the sediment (Y axis).
1031 The contribution of the major taxa is expressed as mean of specimens observed in each
1032 layer (X axis). For macrofauna and metazoan meiofauna, the group 'others' includes all taxa
1033 representing less than 2% and 0.5%, respectively, of the community.

1034 Fig. 3 Richness and abundance of macrofauna, metazoan meiofauna and foraminifera at the
1035 two studied sites, inside a pockmark (Site 1; blue) and away from a pockmark field (Site 2;
1036 yellow). Boxplots of macrofaunal, metazoan meiofaunal and foraminifera richness are based
1037 on the number of high-taxonomic-levels/groups. Y-axes indicate values of richness (high-
1038 taxonomic-levels/groups) and abundance (number of specimens) measures considering all
1039 the cores of each benthic component (sampling area for macrofauna: 0.018 m²; sampling
1040 area for meiofauna: 30 cm²). Boxplots depict the median value (horizontal line in the box),
1041 the distributions of 50% of the data (the box), and the highest and lowest values within 95%
1042 of the distribution (the whisker).

1043 Fig. 4 Principal component analysis (scaling 2) biplots based on Hellinger-transformed data
1044 on taxon composition of each community (macrofauna, metazoan meiofauna and
1045 foraminifera) and their dominant taxa (Polychaeta, Nematoda, hyaline foraminifera) at the
1046 two study sites, inside a pockmark (Site 1; red) and away from another pockmark field (Site
1047 2; blue). Passive (*post hoc*) explanations of axes using environmental variables (DO,
1048 dissolved oxygen; S, total sulfur; and C, organic carbon concentrations) were conducted to
1049 find factor averages of the studied environmental variables.

1050 Fig. 5 Polychaeta, Nematoda and hyaline foraminifera community structure characterizing
1051 the uppermost sediment layer (0-1 cm) at the two study sites. Taxon contribution is
1052 expressed as mean of specimens (abundance of each Nematoda genus was estimated
1053 based on subsample data) (Y axis). The group 'others', in black, includes all taxa whose
1054 presence is limited to 1 or 2 Polychaeta specimens (Site 1: 1 family; Site 2: 7 families); less
1055 than 2% of total Nematoda community (Site 1: 23 genera; Site 2: 59 genera); and 4% of total
1056 foraminifera community (Site 1: 66 species; Site 2: 49 species).

1057 Fig. 6 Richness and abundance of Polychaeta, Nematoda and hyaline foraminifera at the two
1058 study sites, inside a pockmark (Site 1; blue) and away from a pockmark field (Site 2; yellow).
1059 Y-axes indicate values of richness (families, genera and species, respectively) and
1060 abundance (number of specimens) measures considering all the cores of each benthic
1061 component (sampling area for macrofauna: 0.018 m²; sampling area for meiofauna: 30 cm²).
1062 Boxplots represent the median value (horizontal line in the box), the distributions of 50% of

1063 the data (the box), and the highest and lowest values within 95% of the distribution (the
1064 whisker).

1065

1066 **ANNEXES**

1067 Annex I. Depth profiles of oxygen (O_2), methane (CH_4), organic carbon (OC), total sulfur (S)
1068 and hydrogen sulfide (H_2S) content at the two study sites.

1069 Annex II. Richness and abundance values of macrofaunal, metazoan meiofaunal and
1070 foraminifera communities along the vertical profile at both sites (Site 1 and Site 2, inside a
1071 pockmark and away from a pockmark field, respectively). Columns represent median values
1072 and whiskers illustrate the highest and lowest values within 95% of the distribution. Changes
1073 in total sulfur and dissolved oxygen concentrations along the vertical profile are illustrated in
1074 red and green, respectively. Concentrations of total sulfur and dissolved oxygen are
1075 expressed in µmol/L.

1076

1077 Annex III. Results of the inter-site statistical analyses for the macrofaunal, meiofaunal and
1078 foraminifera communities. P-value < 0.05 in the GLMs indicates that the factor "site" has
1079 effect on the response variables (richness and abundance of macro-, meiofauna, and
1080 foraminifera, abundance of taxonomic groups, as well as for their dominant taxa, Polychaeta,
1081 Nematoda, and hyaline foraminifers) (P, p-value; S, t-value and z-value reported by the 'glm',
1082 'lmer' and 'glmer' functions; E, estimate). PERMANOVA shows differences in community
1083 composition inside and away from a pockmark field (Site 1 and Site 2) when p-value < 0.05
1084 (differences are analyzed in terms of abundance of macro-, meiofauna and foraminifera, as
1085 well as for their dominant taxa, Polychaeta, Nematoda, and hyaline foraminifers) (P, p-value;
1086 F, F-model; R^2, explained variance). Results statistically significant are highlighted in bold.

	INTER-SITE					
	GLMs			PERMANOVA		
	P	S	E	P	F	R^2
MACROFAUNA						
Richness	**0.00596**	2.750	0.5845			
Abundance	**0.02100**	3.691	0.4500	**0.005**	2.5763	0.09015
Taxon abundance:						
Polychaeta	**0.00453**	2.874	0.4379			
Cumacea	**0.00554**	3.047	2.034e-01			
Tanaidacea	**0.00224**	3.421	0.29424			
Amphipoda	**0.0317**	2.609	0.16819			

POLYCHAETA						
Richness	0.578	0.556	0.2076			
Abundance	0.27300	-1.270	-0.3613			
Taxon abundance: Hesionidae	**3.23e-06**	-36.87	-0.82278			
MEIOFAUNA						
Richness	**0.0402**	-2.052	-0.3210			
Abundance	**0.005923**	-3.032	-0.5553	**0.019**	2.8249	0.098
Taxon abundance: Nematoda	**0.006780**	-2.974	-0.5744			
Kinorhyncha	**0.00535**	-5.365	-0.9229			
NEMATODA						
Richness	**7.8e-05**	3.95	0.7361			
Abundance	0.076389	-2.659	-0.7929			
Taxon abundance:						
Desmodora	**0.000215**	-21.68	-2.9433			
Pselionema	**0.00916**	6.027	1.127e+00			
FORAMINIFERA						
Richness	0.3061	1.023	0.2288			
Abundance	0.75945	-0.350	-0.04639	0.142	1.7543	0.05225
Group abundance:						
Soft-shell	**0.0423**	2.124	0.09843			
HYALINE						
Richness	0.268	-1.108	-0.1643			
Abundance	0.32550	-1.292	-0.2496			
Taxon abundance:						
U. semiornata	**0.00996**	9.946	1.4978			
B. alata	**0.0270**	-5.960	-2.1099			
B.spathulata (type 2)	**0.00615**	-12.70	-1.6483			
B. inflata	**0.0438**	-4.618	-1.2694			

1087

1088

1089

1090 Annex IV. Differential interference contrast photograph of epifaunal protists on a *Desmodora*
1091 specimen (Nematoda).

a
Atlantic ocean
Indian ocean

b

c
Acoustic anomaly (related to escaping gas bubbles)
Pockmark (Site 1)
Bathymetry (m)
EM122-12 kHz
10 m pixel grid
-2000   -630
0   1000 m

Bathymetry
-80 m
-2800 m

0 2,5 5   10
Km

Site 1 ★
Site 2 ★

Site 1

d
MTB - 6   MTB - 7
KGS-3
0   1   2   4 Km

Site 2

e
KGS-1
MTB-1
0   1   2   4 Km
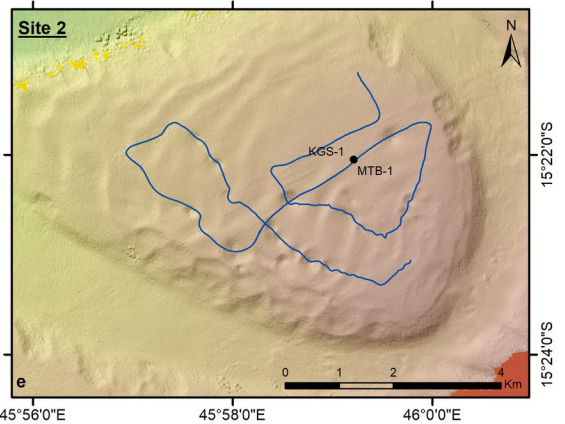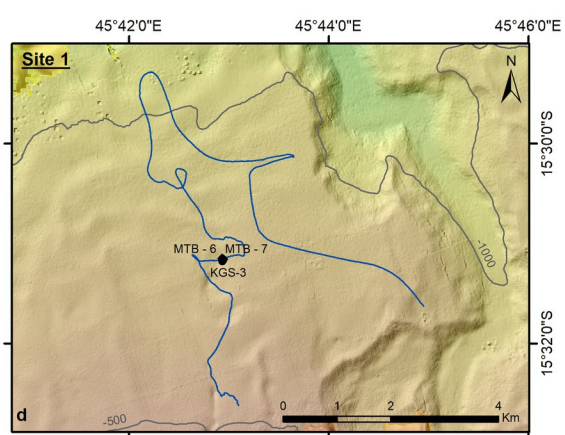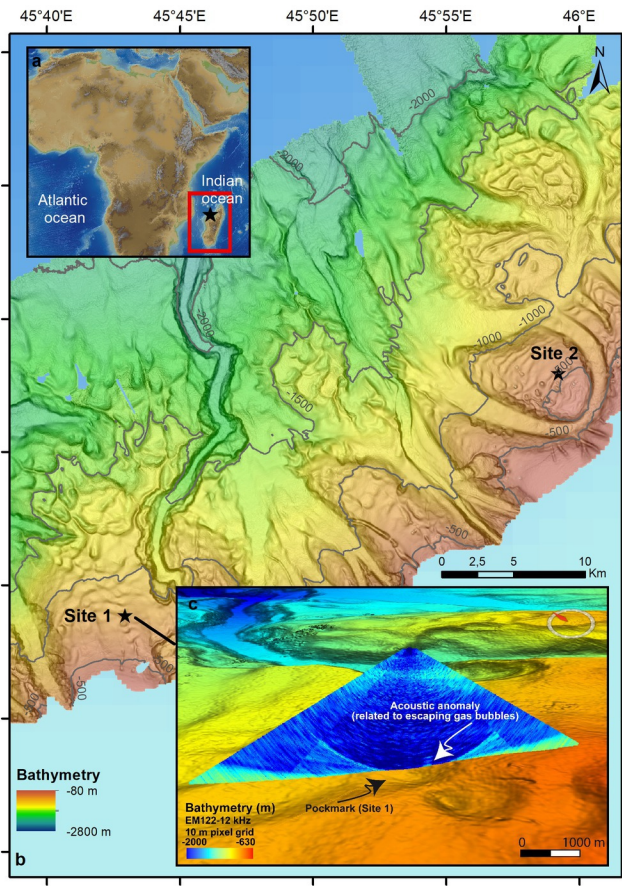
	OUTSIDE POCKMARK	INSIDE POCKMARK

MACROFAUNA

Depth intervals (cm): 0–1, 1–3, 3–5, 5–10, 10–15
Scale: 50, 40, 30, 20, 10, 0 (outside) / 0, 10, 20, 30, 40, 50 (inside)

Legend: Polychaeta, Isopoda, Cumacea, Tanaidacea, Amphipoda, Aplacophora, Bivalvia, Nemertea, Others

MEIOFAUNA

Depth intervals (cm): 0–1, 1–2, 2–3, 3–4, 4–5
Scale: 3000, 2500, 2000, 1500, 1000, 500, 0 (outside) / 0, 500, 1000, 1500, 2000, 2500, 3000 (inside)

Legend: Nematoda, Copepoda, Kinorhyncha, Nauplii, Polychaeta, Bivalvia, Others

FORAMINIFERA

Depth intervals (cm): 0–1, 1–2, 2–3, 3–4, 4–5, 5–6, 6–7, 7–8, 8–9, 9–10
Scale: 1400, 1200, 1000, 800, 600, 400, 200, 0 (outside) / 0, 200, 400, 600, 800, 1000, 1200, 1400 (inside)

Legend: Hyaline, Agglutinated, Porcelaneous, Soft shell

	TOTAL COMMUNITY	DOMINANT TAXON

MACROFAUNA

Macrofauna — PC 1 (54.72%), PC 2 (21.38%); DO, Cumacea, Aplacophora, Nemertea, S C

Polychaeta — PC 1 (47.47%), PC 2 (26.9%); DO, Polynoidae, Hesionidae, Cossuridae, Ophelidae, S, C

MEIOFAUNA

Meiofauna — PC 1 (57.41%), PC 2 (31%); DO, Nauplii, Kinorhyncha, S C

Nematoda — PC 1 (80.9%), PC 2 (17.06%); DO, Tricoma, Pselionema, Desmodora, S C
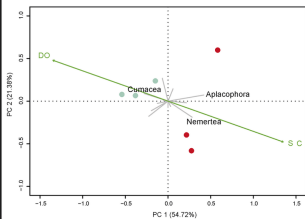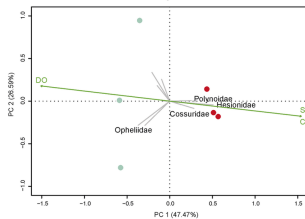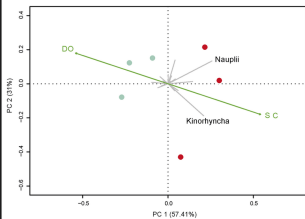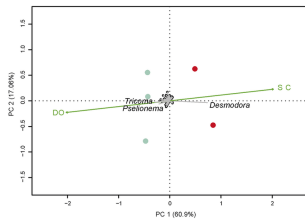
FORAMINIFERA

Foraminifera — PC 1 (81.62%), PC 2 (16.23%); Porcelaneous, Hyaline, Soft-shell, Agglutinated, C, S, DO

Hyaline — PC 1 (73.40%), PC 2 (7.93%); DO, Uvigerina semiornata, Uvigerina hispida, Bolivina inflata, Bolivina spathulata (type 2), Bolivina alata, S, C

POLYCHAETA

- Spionidae
- Hesionidae
- Cossuridae
- Polynoidae
- Capitellidae
- Syllidae
- Opheliidae
- Others

NEMATODA

- *Desmodora*
- *Halalaimus*
- *Tricoma*
- *Desmoscolex*
- *Calligyrus*
- *Chromadorella*
- *Leptolaimus*
- *Chromadorina*
- *Halichoanolaimus*
- *Marylynnia*
- *Prochromadorella*
- *Aegialoalaimus*
- *Chromadorita*
- *Draconema*
- *Elzalia*
- *Innocuonema*
- *Pselionema*
- *Quadricoma*
- *Sabatieria*
- Others

HYALINE

- *B. marginata*
- *B. alata*
- *B. spathulata (2)*
- *U. hispida*
- *B. inflata*
- *U. semiornata*
- *R. lepida*
- *B. spathulata (1)*
- Others

Table 1. Position of sampling: Site 1, active pockmark on the Mahavavy Sud slope; Site 2, outside another pockmark field on the Betsiboka slope.

Site	Location	Latitude (S)	Longitude (E)	Depth (m)	Cruise label	Gear	Date (dd/mm/yy)
Site 1	Inside the pockmark	15° 31,1748'	45° 42,93384'	775	MOZ01-KGS03	USNEL box	07/10/2014
		15° 31,14888'	45° 42,9309'	789	MOZ01-MTB06	Barnett-type multi-corer	07/10/2014
		15° 31,1559'	45° 31,1559'	776	MOZ01-MTB07	Barnett-type multi-corer	07/10/2014
Site 2	Ouside the pockmark field	15° 22,05054'	45° 22,05054'	528	MOZ01-KGS01	USNEL box	04/10/2014
		15° 22,04772'	45° 22,04772'	529	MOZ01-MTB01	Barnett-type multi-corer	04/10/2014

Table 2. Number of taxonomic groups (richness) and number of specimens (abundance) of macrofauna, meiofauna and foraminifera present in the pockmark (Site 1) and away from a pockmark field (Site 2). Data are given for each core and layer along the vertical profile. X gives the mean values ± standard deviation.

		Sediment layer	SITE 2 MOZ01 KGS01/ MTB01				SITE 1 (pockmark) MOZ01 KGS03/ MTB06/MTB07			
			A	B	C	X	A	B	C	X
MACROFAUNA	Richness	0-1	6	7	5	6 ± 1	5	5	6	5.33 ± 0.58
		1-3	6	6	4	5.53 ± 1.15	3	3	0	2 ± 1.73
		3-5	5	4	4	4.33 ± 0.58	1	2	1	1.33 ± 0.58
		5-10	3	3	2	2.66 ± 0.58	1	2	2	1.66 ± 0.58
		10-15	2	2	2	2 ± 0	0	1	2	1 ± 1
	Abundance	0-1	27	26	37	30 ± 6	40	74	21	45 ± 26.85
		1-3	22	52	23	32 ± 17	6	8	0	4.66 ± 4.16
		3-5	19	10	14	14 ± 5	1	5	1	2 ± 2.31
		5-10	33	11	15	20±12	2	11	6	6.33 ± 4.51
		10-15	4	3	3	3 ± 0.6	0	1	4	1.66 ± 2.08
MEIOFAUNA	Richness	0-1	6	7	12	8.33 ± 3.21	-	12	7	9.5 ± 3.54
		1-2	8	7	9	8 ± 1.00	8	8	9	8.33 ± 0.58
		2-3	6	6	4	5.33 ± 1.15	6	8	10	8 ± 2.00
		3-4	3	4	4	3.66 ± 0.58	5	2	5	4 ± 1.73
		4-5	0	2	1	1 ± 1.00	2	3	7	4 ± 2.65
	Abundance	0-1	199	374	336	303 ± 92	-	3841	740	2291 ± 2193
		1-2	1030	940	1778	1249 ± 460	1225	737	6476	2813 ± 3182
		2-3	756	1078	521	785 ± 279	735	560	1686	994 ± 606
		3-4	222	323	281	275 ± 51	571	497	416	495 ± 77
		4-5	0	90	1	30 ± 52	267	224	147	212 ± 60
FORAMINIFERA	Richness	0-1	102		99	100 ± 2	67		121	94 ± 38
		1-2	38		49	43 ± 8	36		41	39 ± 4
		2-3	25		28	26.5 ± 2	15		18	17 ± 2
		3-4	17		15	16 ± 1	11		5	8 ± 4
		4-5	18		6	12 ± 8	6		2	4 ± 3
		5-6	13		1	7 ± 9	4		1	2.5 ± 2.12
		6-7	2		1	1.5 ± 0.7	3		0	1.5 ± 2.1
		7-8	2		1	1.5 ± 0.7	3		0	1.5 ± 2.1
		8-9	1		1	1 ± 0	4		0	2 ± 2.8
		9-10	1		0	0.5 ± 0.7	0		0	0
	Abundance	0-1	603		616	609 ± 9	626		2024	1325 ± 988
		1-2	129		96	113 ± 23	460		544	502 ± 59
		2-3	55		67	61 ± 9	78		83	80 ± 4
		3-4	30		22	26 ± 6	17		33	25 ± 11
		4-5	28		7	17.5 ± 14.8	12		19	15.5 ± 4.9
		5-6	13		1	7 ± 9	4		1	2.5 ± 2.1
		6-7	2		1	1.5 ± 0.7	3		0	1.5 ± 2.1

7-8	3	1	2 ± 1.4	3	0	1.5 ± 2.1
8-9	1	1	1 ± 0	4	0	2 ± 2.8
9-10	1	0	0.5 ± 0.7	0	0	0

Table 3. Total macrofauna *sensu stricto* taxa collected at both sites. Abundance of each taxonomic group is given for each core. Total abundance shows number of specimens for each core. Total richness shows number of taxonomic groups for each core. X gives the mean values ± standard deviation. Cores A, B, C in Site 2 (away from a pockmark field) correspond to cores 1, 2, 3 respectively of the sampling campaign. Cores A, B, C in Site 1 (inside the pockmark) correspond to cores 9, 10, 11, respectively, of the sampling campaign.

MACROFAUNA TAXA	SITE 2 MOZ01KGS01				SITE 1 (pockmark) MOZ01KGS03			
	A	B	C	X	A	B	C	X
Amphipoda	9	3	5	5.67 ± 3.06	0	2	2	1.33 ± 1.15
Aplacophora	0	2	3	1.67 ± 1.53	15	13	2	10.00 ± 7.00
Astacidae	1	0	0	0.33 ± 0.58	0	0	0	0.00
Bivalvia	3	5	0	2.67 ± 2.52	5	9	2	5.33 ± 3.51
Cumacea	8	4	4	5.33 ± 2.31	0	0	0	0.00
Gastropoda	0	1	1	0.67 ± 0.58	0	0	2	0.67 ± 1.15
Halacarida	1	0	0	0.33 ± 0.58	0	0	0	0.00
Isopoda	7	15	5	9.00 ± 5.29	5	0	1	2.00 ± 2.65
Mysidacea	1	0	0	0.33 ± 0.58	0	0	0	0.00
Nemertea	0	4	0	1.33 ± 2.31	2	10	5	5.67 ± 4.04
Oligochaeta	0	0	0	0	0	1	0	0.33 ± 0.58
Polychaeta	64	53	64	60.33 ± 6.35	21	50	17	29.33 ± 18.01
Sipunculidae	0	4	0	1.33 ± 2.31	1	0	0	0.33 ± 0.58
Tanaidacea	11	11	10	10.67± 0.58	0	14	1	5.00 ± 7.81
Total abundance	105	102	92	99.67 ± 6.81	49	99	32	60.00 ± 34.83
Total density (ind/1 m^2)	5833	5667	5111	5537 ± 378	2722	5500	1778	3333 ± 1935
Total richness	9	10	7	8.7 ± 1.5	6	7	8	7 ± 1

Table 4. Polychaeta families collected in the 0-1 cm layer at both sites. Abundance of each family is given for each core. Total abundance shows the number of specimens for each core. Total richness shows the number of families for each core. X gives the mean values ± standard deviation. Cores A, B, C from Site 2 (away from a pockmark field) correspond to cores 1, 2, 3, respectively, of the sampling campaign. Cores A, B, C from Site 1 (inside the pockmark) correspond to cores 9, 10, 11, respectively, of the sampling campaign.

POLYCHAETA FAMILY	SITE 2 MOZ01KGS01				SITE 1 (pockmark) MOZ01KGS03			
	A	B	C	X	A	B	C	X
Sigalionidae	1	0	1	0.67 ± 0.58	0	0	0	0.00
Syllidae	3	0	4	2.33 ± 2.08	1	0	0	0.33 ± 0.58
Flabelligeridae	1	0	0	0.33 ± 0.58	0	0	0	0.00
Spionidae	4	1	9	4.67 ± 4.04	6	12	6	8.00 ± 3.46
Sphaerodoridae	2	0	0	0.67 ± 1.15	0	0	0	0.00
Opheliidae	0	1	4	1.67 ± 2.08	0	0	0	0.00
Pilargidae	0	0	0	0.00	0	0	1	0.33 ± 0.58
Cossuridae	0	0	0	0.00	0	11	1	4.00 ± 6.08
Serpulidae	0	1	1	0.67 ± 0.58	0	0	0	0.00
Hesionidae	0	0	0	0.00	6	5	6	5.67 ± 0.58
Onuphidae	0	0	1	0.33 ± 0.58	0	0	0	0.00
Trichobranchidae	0	0	1	0.33 ± 0.58	0	0	0	0.00
Maldanidae	0	0	1	0.33 ± 0.58	0	0	0	0.00
Capitellidae	0	0	0	0.00	0	5	0	1.67 ± 2.89
Polynoidae	0	0	0	0.00	4	4	0	2.67 ± 2.31
Total abundance	11	3	22	12.00 ± 9.54	17	37	14	22.67 ± 12.50
Total density (ind/1m^2)	611	167	1222	667 ± 530	944	2056	778	1259 ± 695
Total richness	5	3	8	5.33 ± 2.52	4	5	4	4.33 ± 0.58

Table 5. Total meiofauna taxa collected at both sites. Abundance of each taxonomic group is given for each core. Total abundance shows the number of specimens for each core. Total richness shows the number of taxonomic groups for each core. X gives the mean values ± standard deviation. Cores A, B, C from Site 2 (away from a pockmark field) and Site 1 (inside) the pockmark correspond to cores 1, 2, 3 of both sites, respectively, of the sampling campaign.

MEIOFAUNA TAXA	SITE 2 MOZ01MTB01				SITE 1 (pockmark) MOZ01MTB06			
	A	B	C	X	A	B	C	X
Amphipoda	0	0	0	0.00	4	3	1	2.7 ± 1.5
Aplacophora	0	0	0	0.00	4	3	8	5 ± 3
Bivalvia	0	0	1	0.3 ± 0.6	4	31	55	30 ± 26
Cnidaria	0	0	0	0.00	0	2	0	0.7 ± 1.2
Copepoda	122	127	162	137 ± 22	71	368	642	360 ± 286
Cumacea	0	0	2	0.7 ± 1.6	0	1	1	0.7 ± 0.6
Gastropoda	0	0	0	0.00	0	7	2	3.0 ± 3.6
Halacarida	0	0	0	0.00	0	0	1	0.3 ± 0.6
Isopoda	3	0	0	1.0 ± 1.7	0	0	0	0.00
Kinorhyncha	4	14	12	10.0 ± 5.3	115	64	315	165 ± 132
Nauplii	4	0	27	10 ± 14	9	188	228	142 ± 117
Nematoda	2028	2611	2668	2436 ± 354	2568	5116	8124	5269 ± 2781
Ostracoda	10	8	3	7.0 ± 3.6	2	24	53	26 ± 26
Platyhelminthes	0	4	0	1.3 ± 2.3	0	0	0	0
Polychaeta	31	38	27	32.0 ± 5.6	21	44	26	30 ± 12
Tanaidacea	4	1	1	2.0 ± 1.7	0	8	8	5.3 ± 4.6
Tantulocarida	0	1	1	0.7 ± 0.6	0	0	0	0
Tardigrada	1	1	13	5.0 ± 6.9	0	0	1	0.3 ± 0.6
Total abundance	2207	2805	2917	2643 ± 382	2798	5859	9465	6041 ± 3337
Total density (ind/10cm^2)	731	929	966	875 ± 126	927	1941	3135	2001 ± 1105
Total richness	9	9	11	9.7 ± 1.2	9	13	14	12.0 ± 2.7

Table 6. Nematoda genera collected in the 0-1 cm layer at both sites. Nematodes from subsamples were first identified and the final contribution of each genus to the total nematode abundance was then estimated (estimated values are shown as "ca."). Abundance of each genus is given for each core. Total abundance shows the number of specimens for each core. Total richness shows the number of genera for each core. X gives the mean values ± standard deviation. Cores A, B, C from Site 2 (away from a pockmark field) and Site 1 (inside) the pockmark correspond to cores 1, 2, 3 of both sites, respectively, of the sampling campaign.

NEMATODA GENUS	SITE 2 MOZ01MTB01				SITE 1 (pockmark) MOZ01MTB06		
	A	B	C	X	B	C	X
Actinonema	0	4	7	3.7 ± 3.5	0	0	0
Aegialoalaimus	4	11	0	5.00± 5.6	31	0	16 ± 22
Ammotheristus	0	2	3	1.7 ± 1.5	0	0	0
Araeolaimus	1	0	0	0.3 ± 0.6	31	0	16 ± 22
Amphimonhystrella	1	0	0	0.3 ± 0.6	31	0	16 ± 22
Calligyrus	10	9	7	8.7 ± 1.5	0	0	0
Chromadorella	10	2	0	4.0 ± 5.3	93	0	47 ± 66
Chromadorita	3	15	7	8.3 ± 6.1	62	0	31 ± 44
Chromadorina	0	2	0	0.7 ± 1.2	124	0	62 ± 88
Cyartonema	1	2	0	1.0 ± 1.0	0	6	3 ± 4
Cyatholaimus	0	0	3	1.0 ± 1.7	31	0	16 ± 22
Comesomoides	0	0	0	0	62	0	31 ± 44
Daptonema	1	6	0	2.3 ± 3.2	0	0	0
Desmodora	0	0	0	0	1334	576	955 ± 536
Desmodorella	6	2	3	3.7 ± 2.1	0	0	0
Desmoscolex	19	15	27	20 ± 6	31	6	19 ± 18
Diplopeltoides	0	4	3	2.3 ± 2.1	0	0	0
Diplopeltula	3	0	0	1.0 ± 1.7	0	0	0
Draconema	3	13	7	8 ± 5	0	0	0
Eleutherolaimus	1	2	0	1.0 ± 1.0	0	0	0
Elzalia	4	9	3	5.3 ± 3.2	62	0	31 ± 44
Endeolophos	0	4	0	1.3 ± 2.3	0	0	0
Gnomoxyala	0	2	0	0.7 ± 1.2	31	0	16 ± 22
Halalaimus	9	24	17	17 ± 8	310	0	155 ± 219
Halichoanolaimus	0	0	0	0.00	93	0	47 ± 66
Innocuonema	0	17	10	9.0 ± 8.5	0	6	3 ± 4
Linhystera	1	4	3	2.7 ± 1.5	0	0	0
Leptolaimus	3	9	7	6.3 ± 3.1	124	0	62 ± 88
Longicyatholaimus	1	4	0	1.7 ± 2.1	31	0	16 ± 22
Marylynnia	1	4	0	1.7 ± 2.1	93	0	47 ± 66
Metasphaerolaimus	0	0	3	1.0 ± 1.7	31	6	19 ± 18
Oxystomina	0	2	7	3.0 ± 3.6	0	0	0

Paracomesoma	1	4	3	2.7 ± 1.5	31	0	16 ± 22
Paracyatholaimus	0	2	3	1.7 ± 1.5	0	0	0
Paralongicyatholaimus	0	2	7	3.0 ± 3.6	0	0	0
Parachromadorita	0	6	0	2.0 ± 3.5	31	0	16 ± 22
Paramonohystera	0	2	0	0.7 ± 1.1	31	0	16 ± 22
Parodontophora	0	4	0	1.3 ± 2.3	0	0	0
Pierrickia	1	11	0	4 ± 6	62	0	31 ± 44
Prochromadorella	0	0	0	0.00	93	0	47 ± 66
Pseudodesmodora	4	2	3	3 ± 1	0	0	0
Pselionema	7	11	24	14 ± 9	0	0	0
Quadricoma	0	15	7	7 ± 8	0	6	3 ± 4
Richtersia	0	0	7	2 ± 4	0	0	0
Sabatieria	7	0	7	5 ± 4	62	0	31 ± 44
Spilophorella	1	2	0	1 ± 1	0	0	0
Thalassomonhystera	0	11	0	4 ± 6	62	0	31 ± 44
Terschellingia	1	2	0	1 ± 1	31	0	16 ± 22
Tricoma	16	37	45	33 ± 15	31	0	16 ± 22
Wieseria	0	2	3	1.7 ± 1.5	0	0	0
Undeterminated	0	0	7	2 ± 4	0	0	0
Total id. specimens	95	145	74	105 ± 36	102	104	103 ± 1
Total abundance	141	314	254	236 ± 88	3165	611	1888 ± 1806
Total density (ind/10cm^2)	47	104	84	78 ± 29	1048	202	625 ± 598
Total richness	35	52	32	39.67 ± 10.79	31	7	19 ± 16.97

Remaining taxa were recovered at one of the sites as singletons before estimations of the contribution of each genus to the total community. Singletons at Site 1: *Anoplostoma*, *Cobbia*, *Paralinhomoeus* and *Prochromadora*. Singletons at Site 2: *Achantolaimus*, *Antomicron*, *Apenodraconema*, *Amphimonhystera*, *Anticyathus*, *Bathyeurystomina*, *Belbolla*, *Bolbonema*, *Calyptronema*, *Campylaimus*, *Dasynemoides*, *Dichromadora*, *Graphonema*, *Greeffiella*, *Halomonhystera*, *Linhomoeus*, *Metadesmolaimus*, *Metalinhomoeus*, *Promonhystera*, *Retrotheristus*, *Southerniella*, *Scaptrella*, *Spiliphera*, *Synodontium* and *Theristus*.

Table 7. Total foraminifera taxa collected at both sites. Abundance of each main group and dominant species is given for each core. Total abundance shows the number of specimens for each core. Total richness shows the number of species for each core. X gives the mean values ± standard deviation. Cores A, B from Site 2 (away from a pockmark field) and site 1 (inside) the pockmark correspond to cores 1, 2 at both sites, respectively, of the sampling campaign.

FORAMINFERA TAXA	SITE 2 MOZ01MTB01			SITE 1 (pockmark) MOZ01MTB07		
	A	B	X	A	B	X
Hyaline	524	527	526 ± 2	758	1459	1109± 496
B. marginata	80	93	86 ± 9	139	371	255 ± 164
B. alata	0	0	0	252	520	386 ± 190
G. barbata	19	10	14 ± 6	1	1	1 ± 0
U. semiornata	51	54	53 ± 2	2	1	1.5 ± 0.71
Agglutinated	286	237	262 ± 35	434	1161	798 ± 514
H. bradyi	0	0	0	94	221	158 ± 90
N. compressa	0	0	0	157	372	265 ± 152
Porcelaneous	41	30	36 ± 8	11	72	42 ± 43
Soft shell	14	18	16 ± 3	4	12	8 ± 6
Total abundance	865	812	839 ± 37	1207	2704	1956 ± 1058
Total density (ind/10cm^2)	123.83	114.37	118 ± 5	170.00	380.85	275 ± 149
Total richness	80	114	97 ± 24	124	123	123.5 ± 0.7

Table 8. Hyaline foraminifer species collected in the 0-1 cm layer at both sites. See Fontanier et al (2016) for detailed information on the reported data. Abundance of each species is given for each core. Total abundance shows the number of specimens for each core. Total richness shows the number of species for each core. X gives the mean values ± standard deviation. Cores A, B from Site 2 (away from a pockmark field) and Site 1 (inside) the pockmark correspond to cores 1, 2 at both sites, respectively, of the sampling campaign.

HYALINE SPECIES	SITE 2 MOZ01MTB01			SITE 1 (pockmark) MOZ01MTB07		
	A	B	X	A	B	X
Bolivina alata	0	0	0	56	290	173 ± 165
Bolivina spathulata (type 1)	11	21	16 ± 7	18	25	22 ± 5
Bolivina spathulata (type 2)	0	0	0	32	59	46 ± 19
Bolivinita quadrilatera	1	1	1 ± 0	18	14	16 ± 3
Bulimina inflata	4	1	2.5 ± 2.1	90	37	64 ± 38
Bulimina marginata	62	75	69 ± 9	106	310	208 ± 144
Cassidulina laevigata var. carinata	5	5	5 ± 0	8	14	11 ± 4.24
Cibicides bradyi	8	5	6.5 ± 2.1	1	3	2 ± 1
Cibicidoides kullenbergi	8	0	4 ± 6	4	8	6 ± 3
Cibicidoides pachydermus/kullenbergi	4	9	6.5 ± 3.5	0	0	0
Cibicidoides ungerianus	3	9	6 ± 4.2	0	0	0
Hoeglundina elegans	9	16	13 ± 5	8	20	14 ± 8
Lenticulina sp.1	3	7	5 ± 3	1	1	1 ± 0
Lenticulina peregrina	0	1	0.5 ± 0.7	7	16	12 ± 6
Nuttallides rugosus	12	8	10 ± 3	3	5	4 ± 1
Pullenia sp.2	0	0	0	0	16	8 ± 11
Pullenia bulloides	2	1	1.5 ± 0.7	18	19	18.5 ± 0.7
Rotorbinella lepida	18	25	22 ± 5	1	6	3.5 ± 3.5
Siphogenerina columellaris subs. costulata	10	15	13 ± 4	4	1	2.5 ± 2.1
Siphonina reticulata	9	2	6 ± 5	0	0	0
Trifarina bradyi	7	12	9.5 ± 3.5	1	1	1 ± 0
Uvigerina hispida	46	94	70 ± 34	10	65	38 ± 39
Uvigerina semiornata	44	43	43.5 ± 0.7	0	1	0.5 ± 0.7
Total abundance*	347	410	379 ± 45	433	1039	736 ± 429
Total density (ind/10 cm^2)*	48.87	57.75	53 ± 6	60.99	146.34	104 ± 60
Total richness*	40	44	42 ± 3	39	60	50 ± 15

Remaining taxa represent less than 1% of the total hyaline community at both sites. Total abundance, total density, and total richness include all the taxa observed in the samples